Technical report; TR-245

KNMI

A comprehensive description of the KNMI seismological instrumentation

Bernard Dost and Hein Haak

De Bilt, 2002

Technical Report = Technisch Rapport; TR-245

De Bilt, 2002

PO Box 201, 3730 AE De Bilt
The Netherlands
Wilhelminalaan 10
http://www.knmi.nl
Telephone +31 30 22 06 911
Telefax +31 30 22 10 407

Authors: Dost, Bernard
Haak, Hein

UDC: 550.34
550.34.03
550.34.037
354.4.075.5KNMI
(492)

ISSN: 0169-1708

ISBN: 90-369-2212-7

A comprehensive description of the KNMI seismological instrumentation

Bernard Dost and Hein Haak

Royal Netherlands Meteorological Institute
July 2002

Contents

1. Introduction

The basic dataset for observational seismological research is an archive of analogue and digital seismograms. The information content of these seismograms is viewed as a convolution of a source wavelet with a Green's function, followed by a convolution with the instrument response. Only if the instrument response is known accurately and can be corrected for, inferences on the structure of the earth and the mechanism of earthquakes can be made.

Although calibration of the instrumentation used to be an important task, this information was of limited use before the introduction of digital recording. A diagram of the amplification as a function of frequency was regarded sufficient. With the introduction of digital recording, however, the instrument response could be removed from the recorded waveforms and other recording systems simulated (e.g. Wood-Anderson seismograph), allowing a more complete analysis of the waveforms (Seidl, 1980). At the same time a greater diversity in instrumentation was introduced, since the traditional galvanometer was replaced by one or more anti-aliasing filters (electronics). No general rule for the steepness of these filters or their shape was formulated, although Butterworth filters are mostly chosen because of their behaviour (the amplitude behaviour is maximally flat in the chosen frequency band). Due to this diversity in instrumentation and the freedom to make modifications to the existing measurement systems there is an urgent need to document existing instrumentation and keep track of modifications in time.

The purpose of this technical report is to give a description of instrumentation installed and maintained by the KNMI in de Bilt in a comprehensive manner. The description is given in the form of transfer functions, which characterize the measurement systems in the frequency domain. Based on these transfer functions, recursive time domain filters are developed. These filters are used to correct for instrument response and convert either velocity- or acceleration data into ground displacement. This enables a check on the description of the instrumentation. A description of these filters and their performance will be the subject of a separate Technical Report (TR).

The focus will be on modern digital instrumentation. However, since digitisation of analogue recordings of mainly the Galitzin seismograph in de Bilt is a present issue, also the transfer function of the analogue systems will be presented. A separate issue is the timing of the seismograph systems. Different timing systems are used and will be briefly discussed.

It is the intention to regularly update this technical report.

Figure 2.1. Overview of seismic stations in the Netherlands, installed and maintained by the KNMI (status: summer 2002). Broad-band stations are shown as filled triangles.

2. Broad-band instrumentation

Broad-band stations **HGN** and **WIT** are in operation since 1993. The first year in an experimental stage, since 1994 fully operational. Continuous digital data of these stations are available at the KNMI. The seismic sensor used in **WIT** is an STS-1 Broad-Band (BB) seismograph (Wielandt and Streckeisen, 1982), while station **HGN** is equipped with a Very Broad-Band (VBB) version of the STS-1. The VBB sensor is described in the literature by Wielandt and Steim (1985) and in the documentation provided by the manufacturer. For details concerning the design and operation of seismic sensors the reader is referred to Wielandt (2001).
The STS-1 acts as a second-order high-pass filter for velocity. Due to the applied feedback a second order low-pass filter is added for the higher frequencies. The difference between the BB and VBB sensors is their eigenperiod (BB: 20s; VBB: 360s) and their high frequency cut-off (BB: 5 Hz; VBB: 10 Hz). The station electronics (predominantly anti-alias filters and A/D conversion) is made after the instrumentation of the Graefenberg array with minor modifications. In total a 7th order low-pass filter is designed. A description of this system is given by Seidl and Stammler (1984).

Station **WTSB** is an upgrade of short period station **WTS**, in a slightly different location. The sensor used is an STS-2, characterized by an eigenperiod at 120 s and a flat frequency response, with respect to velocity, at higher frequencies (up to app. 30 Hz). Although for most teleseismic studies the detailed high frequency behaviour of the sensor is not important, the sensor is also used for local and regional studies and data are sampled at relatively high sampling rates (40-100 Hz). Therefore this document will also provide details on the high frequency behaviour of the STS-2 sensor, which is produced in three generations.

Finally, the first of a new generation of broad-band stations, **OPLO**, will be described, equipped with an STS-2 sensor and a state of the art Quanterra 24 bits data logger.

In the description of the transfer function all information is given in the Laplace domain where the parameter $s = i\omega$ plays a central role and $\omega = 2\pi f$ (f = frequency in Hz). All equations describing the transfer functions are given with respect to displacement, while the corresponding figures are all given with respect to velocity.

2.1 *General description*

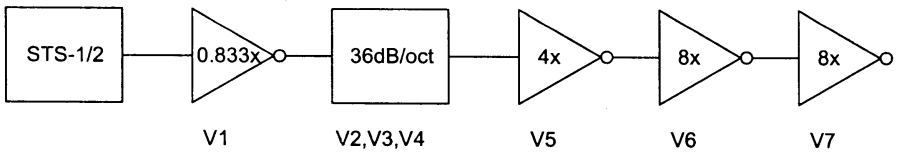

Figure 2.2: Schematic overview of the first generation station electronics for ***HGN, WIT and WTSB***

The first generation electronics developed for broad-band stations **HGN, WIT** and **WTSB** all share the same components as shown in figure **2.2**. Small differences in electronics and sensor are discussed in sections **2.2-2.4**, where station details are presented. Limited dynamic range, caused by the 16 bit A/D conversion, was extended by applying gain-ranging (section V5-V7). However, this gain ranging introduced transients in the digitisation process. In addition, the steep analogue anti-alias filter (section V2-V4) caused an apparent time delay, especially in combination with a low signal to noise ratio. Both drawbacks of the first generation electronics were taken into account by selecting the next generation.

The second generation did not involve specially designed hardware, but instead used commercially available hardware. It was decided to standardize on a Quanterra datalogger in combination with STS-1 or -2 sensor. The Quanterra combines a 24 bit digitiser with digital Finite Impulse Response (FIR) anti-alias filters. As a consequence station **OPLO** operates from the start without the amplification (V1), anti-alias filter (V2-V4) or gain-ranging (V5-V7) stages shown in figure **2.2**. Station **OPLO** was the first (prototype) station that operated in a triggered mode and could be accessed by modem. The other stations are equipped with a dedicated phone line and continuous data are stored in a digital archive at de Bilt.

Due to a further modernisation of the recording systems, all broad-band stations will operate in the near future (2002-2003) with a Quanterra datalogger, replacing the older electronics.

2.1.1 *Broad-band seismographs*

The transfer function of the **STS-1** sensor for displacement is given by (Seidl and Stammler, 1984):

$$T_s(s) = \frac{s^3 S}{s^2 + 2h_0\omega_0 s + \omega_0^2} \cdot \frac{(s+a_1)\omega_1^2}{s^2 + 2h_1\omega_1 s + \omega_1^2} \qquad 1.1$$

where S is the sensitivity in Vs/m, h_0 damping and a_1 a corner frequency in rad/s. This response function is identical to that of a conventional seismometer/galvanometer system with zero coupling, if the term $(s+a_1)$ is compensated by the addition of a first order low pass filter at a cut-off corner frequency $s=-a_1$. The response function then becomes:

$$T_s(s) = \frac{s^3 S}{s^2 + 2h_0\omega_0 s + \omega_0^{\,2}} \cdot \frac{\omega_1^{\,2}}{s^2 + 2h_1\omega_1 s + \omega_1^{\,2}} \qquad 1.2$$

or:

$$T_s(s) = \frac{s^3 S}{(s-s_1)(s-s_2)} \cdot \frac{\omega_1^{\,2}}{(s-s_3)(s-s_4)}, \text{ with} \qquad 1.3$$

$$s_{1,2} = -h_0\omega_0 \pm i\omega_0\sqrt{1-h_0^{\,2}} \text{ and } s_{3,4} = -h_1\omega_1 \pm i\omega_1\sqrt{1-h_1^{\,2}}$$

In case of the STS-1 BB sensor, ω_0 =0.314 rad/s (f_0 = 0.05 Hz) and ω_1 = 31.42 rad/s (f_1 = 5 Hz). For the VBB sensor ω_0 = 0.01745 rad/s (f_0 = 0.00278 Hz) ω_1 = 62.83 rad/s (f_1 = 10 Hz) . For the damping parameters the values are: h_0 = 0.707 , h_1 = 0.623.

For the **STS-2** sensor the low frequency response is (operation manual):

$$T_s(s) = \frac{s^3 S}{s^2 + 2h_0\omega_0 s + \omega_0^{\,2}} \qquad 1.4$$

with $\omega_0 = \frac{2\pi}{120}$ = 0.05236 rad/s and h_0 = 0.707. The velocity response is approximately flat up to 30 Hz (STS-2 manual). The high frequency behaviour of the sensor was revised in time by the manufacturer and comes in three generations. These revisions are totally determined by the electronics, not the sensor (Streckeisen 2001, pers. comm.).

The first generation has a total transfer function:

$$T_s(s) = \frac{s^3 S}{s^2 + 2h_0\omega_0 s + \omega_0^{\,2}} \cdot \frac{A\prod_{k=0}^{2}(s-z_k)}{\prod_{l=0}^{5}(s-p_l)(s-\omega_m)} \qquad 1.4.1$$

the second generation:

$$T_s(s) = \frac{s^3 S}{s^2 + 2h_0\omega_0 s + \omega_0^{\,2}} \cdot \frac{A\prod_{k=0}^{6}(s-z_k)}{\prod_{l=0}^{10}(s-p_l)(s-\omega_m)} \qquad 1.4.2$$

and the third generation:

$$T_s(s) = \frac{s^3 S}{s^2 + 2h_0\omega_0 s + \omega_0^{\,2}} \cdot \frac{A\prod_{k=0}^{3}(s-z_k)}{\prod_{l=0}^{7}(s-p_l)(s-\omega_m)} \qquad 1.4.3$$

with

zeroes	1st generation	2nd generation	3rd generation
z_0	(-318.6, -401.2)	(-5907, -3411)	(-463.1, -430.5)
z_1	(-318.6, 401.2)	(-5907, 3411)	(-463.1, 430.5)
z_2	(-15.15, 0.0)	(-683.9, -175.5)	(-176.6, 0.0)
z_3		(-683.9, 175.5)	(-15.15, 0.0)
z_4		(-555.1, 0.0)	
z_5		(-294.6, 0.0)	
z_6		(-10.75, 0.0)	

poles	1st generation	2nd generation	3rd generation
p_0	(-7454, -7142)	(-6909, -9208)	(-13300, 0.0)
p_1	(-7454, 7142)	(-6909, 9208)	(-10530, -10050)
p_2	(-417.1, 0.0)	(-6227, 0.0)	(-10530, 10050)
p_3	(-100.9, -401.9)	(-4936, -4713)	(-520.3, 0.0)
p_4	(-100.9, 401.9)	(-4936, 4713)	(-374.8, 0.0)
p_5	(-15.99, 0.0)	(-1391, 0.0)	(-97.34, -400.7)
p_6		(-556.8, -60.05)	(-97.34, 400.7)
p_7		(-556.8, 60.05	(-15.64, 0.0)
p_8		(-98.44, -442.8)	
p_9		(-98.44, -442.8)	
p_{10}		(-10.95, 0.0)	

	1st generation	2nd generation	3rd generation
ω_m	-187.24	-255.10	-255.10
A	5.75E12	2.36E17	3.49E17
S	1500	1500	1500

The factor A in equations ***1.4.1-1.4.3*** can be calculated from the poles and (non-zero) zeroes in the table. First, the factors ω_i and h_i are calculated by realising that $s_1 . s_2 = \omega_i^2$ (equation ***1.3***) and the real part of the poles and zeroes is equal to $\omega_i h_i$. The expression for the imaginary part can be used to check the results. Then all factors ω_i, belonging to the filter coefficients but not shown separately in the equations, are multiplied in both the numerator and denominators. An example of this calculation is presented for the 1st generation STS-2:

$z_{0,1}$: $\omega_0 = 512.3$ ($h_0 = 0.622$)

$p_{0,1}$: $\omega_0 = 10323.3$ ($h_0 = 0.722$)

$p_{3,4}$: $\omega_3 = 414.4$ ($h_3 = 0.243$)

$$A = \frac{10323.3^2 \cdot 417.1 \cdot 414.4^2 \cdot 15.99 \cdot 187.24}{512.3^2 \cdot 15.15} = \frac{2.29 \cdot 10^{19}}{3.98 \cdot 10^6} = 5.75 \cdot 10^{12}$$

2.1.2 *Anti-aliasing filters*

Apart from the total gain of the system, that will be addressed in chapter **2.1.4**, the transfer functions of sections V2, V3 and V4 in figure **2.1** are presented. These sections constitute a 5th order anti-aliasing filter (V2 and V3), followed by a 1st order compensation filter. Together with the 2nd order low pass filter of the seismometer, the total system has the form of the desired 7th order low-pass filter. Since the high frequency cut-off is different for the aforementioned seismographs, different settings are required. This will be detailed in the description of the total transfer function (chapter **2.1.3**).

Section V2

In this section the transfer function of a third order anti-aliasing filter is described.

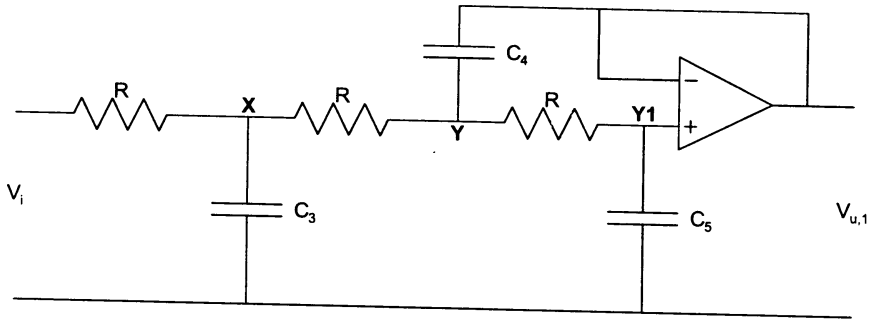

Figure 2.3: Electronics scheme for section V2

Considering the equilibrium of current on points X, Y and Y1 in figure **2.3**, equations are developed relating $V_{u,1}$ to V_{in}:

$$(V_i - V_x)\cdot\frac{1}{R} - V_x C_3 s - (V_x - V_y)\cdot\frac{1}{R} = 0 \qquad \textbf{2.1}$$

$$(V_x - V_y)\cdot\frac{1}{R} + (V_{u,1} - V_y)C_4 s - (V_y - V_{u,1})\cdot\frac{1}{R} = 0 \qquad \textbf{2.2}$$

$$(V_y - V_{u,1})\cdot\frac{1}{R} - V_{u,1} C_5 s = 0 \qquad \textbf{2.3}$$

Using equation **2.3** provides an expression for V_y in terms of $V_{u,1}$:

$$V_y = V_{u,1}(1 + RC_5 s) \qquad \textbf{2.4}$$

Substitution of V_y in equation **2.2** gives:

$$V_x = V_{u,1}(1 + 2RC_5 s + R^2 C_4 C_5 s^2) \qquad \textbf{2.5}$$

And finally, substitution of V_y *and* V_x in equation **2.1** gives:

$$\frac{V_{u,1}}{V_i} = \frac{1}{1 + (3RC_5 + RC_3)s + 2R^2 C_5 (C_3 + C_4)s^2 + R^3 C_3 C_4 C_5 s^3} \qquad \textbf{2.6}$$

The design target is a transfer function of a 3rd order low-pass filter:

$$\frac{V_{u,1}}{V_i} = \frac{1}{(\frac{s}{\omega_1}+1)(\frac{s^2}{\omega_1^2}+\frac{2h_2 s}{\omega_1}+1)} = \frac{1}{\frac{s^3}{\omega_1^3}+(\frac{1+2h_2}{\omega_1^2})s^2+(\frac{1+2h_2}{\omega_1})s+1} \qquad 2.7$$

where ω_1 is determined by the seismometer, which already provides a 2nd order low-pass filter, so using the values of the selected components:

$$\omega_1 = \frac{1}{R}\cdot(\frac{1}{C_3C_4C_5})^{1/3} = 31.42 \text{ rad/s (WIT)}, = 62.84 \text{ rad/s (HGN, WTSB)} \qquad 2.8$$

$$h_2 = R^2C_5(C_3+C_4)\omega_1^2 - \frac{1}{2} = \frac{C_5(C_3+C_4)}{(C_3C_4C_5)^{2/3}} - \frac{1}{2} = 0.901 \qquad 2.9$$

$$h_2 = \frac{R}{2}\cdot(3C_5+C_3)\omega_1 - \frac{1}{2} = \frac{3C_5+C_3}{2(C_3C_4C_5)^{1/3}} - \frac{1}{2} = 0.940 \qquad 2.10$$

Both equations for h_2 should provide the same values, within reasonable error bounds, and determines the ratio between the values of C_3, C_4 and C_5. It is worth noting that the factor h_2 is independent of R, so if there is any need to change ω_1 without influencing the damping, this could be achieved. Since **HGN** and **WIT** do have a difference in value for ω_1 by a factor 2, an adjustment consists only of changing the resistors R by a factor 2.

The final form of the transfer function of section V2 is:

$$T_{v2}(s) = \frac{V_{u,1}}{V_i} = \frac{\omega_1^3}{(s+\omega_1)(s^2+2h_2\omega_1 s+\omega_1^2)} \qquad 2.11$$

Selected components:

Station	R [kΩ]	C_3 [μF]	C_4 [μF]	C_5 [μF]
HGN	5	4.25	4.88	1.56
WTSB	5	4.25	4.88	1.56
WIT	10	4.25	4.88	1.56

Section V3:

The next section is a 2nd order anti-alias filter to complete the 7th order anti-alias filter.

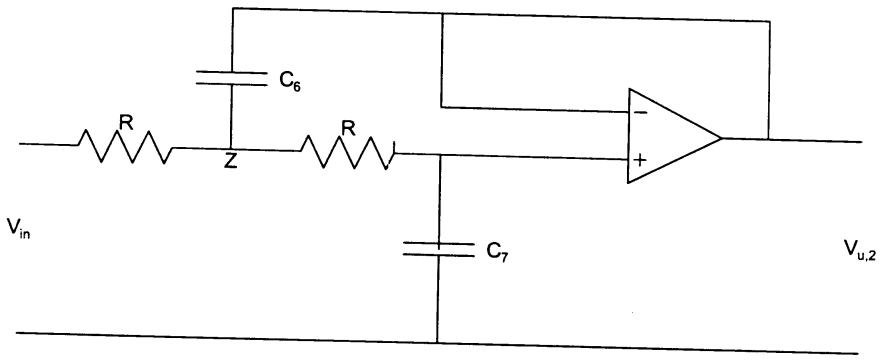

Figure 2.4: Electronics scheme for section V3

In analogy to the previous description, the equations for section V3 are:

$$(V_{in} - V_z)\cdot\frac{1}{R} + (V_{u,2} - V_z)C_6 s - (V_z - V_{u,2})\cdot\frac{1}{R} = 0 \qquad \textbf{2.12}$$

$$(V_z - V_{u,2})\cdot\frac{1}{R} - V_{u,2}C_7 s = 0 \qquad \textbf{2.13}$$

Using equation **2.13** V_z can be expressed in terms of $V_{u,2}$:

$$V_z = V_{u,2}\cdot(1 + RC_7 s) \qquad \textbf{2.14}$$

Substitution of V_z into equation **2.12** leads to:

$$T_{V3}(s) = \frac{V_{u,2}}{V_{in}} = \frac{1}{1 + 2RC_7 s + R^2 C_6 C_7 s^2} = \frac{{\omega_1}^2}{{\omega_1}^2 + 2h_3\omega_1 s + s^2} \qquad \textbf{2.15}$$

From this equivalence the following expressions are derived:

$$\omega_1 = \frac{1}{R}\sqrt{\frac{1}{C_6 C_7}} = 31.43 \text{ rad/s (WIT), } 62.86 \text{ (HGN, WTSB) and}$$

$$h_3 = R\frac{C_7}{\omega_1} = \sqrt{\frac{C_7}{C_6}} = 0.223 \qquad \textbf{2.16}$$

Selected components:

Station	R [kΩ]	C_6 [μF]	C_7 [μF]
HGN	5	14.3	0.708
WTSB	5	14.3	0.708
WIT	10	14.3	0.708

Section V4

This part is the compensation filter for the additional zero in the seismometer response

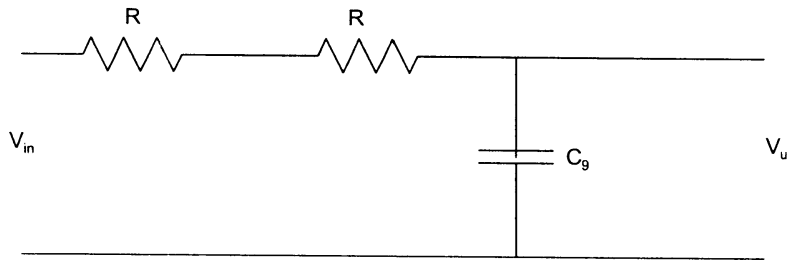

Figure 2.5: Electronics scheme for section V4

The equations for this section are:

$$(V_{in} - V_u) \cdot \frac{1}{2R} + V_u C_9 s = 0 \qquad \textbf{2.17}$$

or

$$T_{V4}(s) = \frac{V_u}{V_{in}} = \frac{1}{1 + 2RC_9 s} = a_1 \cdot \frac{1}{s + a_1} \qquad \textbf{2.18}$$

Where for **WIT** $a_1 = \frac{1}{2RC_9}$ = 42.55 rad/s , which is in accordance to the STS-1 (BB) manual where the recommendation is given to use a value of RC=21 ms (in our case 23.5 ms). For **WTSB** and **HGN** the value for a_1 is a factor 2 higher.

Selected components:

Station	R [kΩ]	C_9 [μF]	a_1 [rad/s]
HGN	10	1.175	85.11
WTSB	10	1.175	85.11
WIT	20	1.175	42.55

2.1.3 *Total transfer function*

Sections V5-V7 only provide a gain to the total system, no frequency dependent amplitude or phase factors and influences only the total sensitivity *S*. For the **STS-1** sensor the total transfer function becomes:

$$T_{tot}(s) = T_s(s) \cdot T_{v2}(s) \cdot T_{v3}(s) \cdot T_{v4}(s)$$

$$T_{tot}(s) = \frac{Ss^3}{(s^2 + 2h_0\omega_0 s + \omega_0^{\,2})} \cdot \frac{\omega_1}{(s+\omega_1)} \cdot \prod_{k=1}^{3} \frac{\omega_1^{\,2}}{s^2 + 2h_k\omega_1 s + \omega_1^{\,2}} \qquad 2.19$$

$$T_{tot}(s) = \frac{Ss^3}{(s-s_1)(s-s_1^{\,*})} \cdot \frac{\omega_1}{(s-s_2)} \cdot \prod_{k=1}^{3} \frac{\omega_1^{\,2}}{(s-s_{k+2})(s-s_{k+2}^{\,*})}$$

In equation **2.19** an asterix (*) is used to indicate complex conjugation. For the poles, a distinction is made between the STS-1 BB (**WIT**) and VBB (**HGN**):

poles	BB (**WIT**)	VBB (**HGN**)
$s_1 = (-\omega_0 h_0, \omega_0 h_0)$	(-0.222, 0.222)	(-0.0123, 0.0123)
$s_2 = (-\omega_1, 0.0)$	(-31.416, 0.000)	(-62.832, 0.000)
$s_3 = (-\omega_1 h_1, \omega_1\sqrt{1-h_1^{\,2}})$	(-19.572, 24.574)	(-39.144, 49.148)
$s_4 = (-\omega_1 h_2, \omega_1\sqrt{1-h_2^{\,2}})$	(-28.306, 13.629)	(-56.612, 27.258)
$s_5 = (-\omega_1 h_3, \omega_1\sqrt{1-h_3^{\,2}})$	(-7.006, 30.625)	(-14.012, 61.250)

A total of 9 poles and 3 zeroes for displacement. The imaginary part of s_1 is equal to the real part, since h_0=0.707.

For the **STS-2** at **WTSB** (2nd generation), the total transfer function becomes:

$$T_{tot}(s) = T_s(s) \cdot T_{v2}(s) \cdot T_{v3}(s) \cdot T_{v4}(s)$$

$$T_{tot}(s) = \frac{Ss^3}{(s^2 + 2h_0\omega_0 s + \omega_0^{\,2})} \cdot \frac{a_1}{(s+a_1)} \cdot \frac{\omega_1}{(s+\omega_1)} \cdot \prod_{k=2}^{3} \frac{\omega_1^{\,2}}{s^2 + 2h_k\omega_1 s + \omega_1^{\,2}} \cdot \frac{A\prod_{k=0}^{6}(s-z_k)}{\prod_{l=0}^{10}(s-p_l)(s-\omega_m)}$$

$$T_{tot}(s) = \frac{Ss^3}{(s-s_1)(s-s_1^{\,*})} \cdot \frac{a_1}{(s-s_5)} \cdot \frac{\omega_1}{(s-s_2)} \cdot \prod_{k=1}^{2} \frac{\omega_1^{\,2}}{(s-s_{k+2})(s-s_{k+2}^{\,*})} \cdot \frac{A\prod_{k=0}^{6}(s-z_k)}{\prod_{l=0}^{10}(s-p_l)(s-\omega_m)} \qquad 2.20$$

Please note that the high frequency part of equation **2.20** is only of interest when a sufficiently high sampling rate is chosen. Figure **2.6** shows the amplitude response for **WTSB**, where the influence of the high frequency part of the sensor is clearly visible. Apart from the poles and zeroes of the high frequency part of the STS-2 (see equation **1.5.2** and following table) the poles are:

poles	**WTSB**
$s_1 = (-\omega_0 h_0, \omega_0 h_0)$	(-0.037, 0.037)
$s_2 = (-\omega_1, 0.0)$	(-62.832, 0.000)
$s_3 = (-\omega_1 h_2, \omega_1 \sqrt{1 - h_2^2})$	(-56.612, 27.258)
$s_4 = (-\omega_1 h_3, \omega_1 \sqrt{1 - h_3^2})$	(-14.012, 61.250)
$s_5 = (-a_1, 0.0)$	(-85.11, 0.000)

2.1.4 *Group delay*

Seidl and Stammler (1984) showed the effect of a steep anti-alias filter on the shape of the leading edge of a step response. Since station **HGN, WIT** and **WTSB** will change its data acquisition part from a system with a steep analog anti-alias filter to a system with only digital filters, it is important to quantify this effect for these stations. This can be done by analysing the group delay

$\tau_G(\omega) = -\dfrac{d\varphi(\omega)}{d\omega}$, where $\phi(\omega)$ is the phase-shift.

The group delay gives the envelope delay of a narrow-band signal and may cause an apparent delay of a certain phase in the seismogram depending on frequency. For **HGN** and **WIT**, the group delay based on equation *2.19* becomes:

$\tau_G(\omega) = \tau_{G0}(\omega) + \tau_{G1}(\omega)$, where subscript G0 stands for the low frequency part of the seismometer response (first part in *2.19*) and G1 for the high frequency part of seismometer and anti-aliasing filter. The individual expressions are:

$$\tau_{G0}(\omega) = \frac{2h_0\omega_0(\omega^2 + \omega_0^2)}{(\omega^2 - \omega_0^2)^2 + 4h_0^2\omega_0^2\omega^2} \qquad 2.21$$

$$\tau_{G1}(\omega) = \frac{\omega_1}{\omega^2 + \omega_1^2} + 2\omega_1 \sum_{k=1}^{3} \frac{h_k(\omega^2 + \omega_1^2)}{(\omega^2 - \omega_1^2)^2 + 4h_k^2\omega_1^2\omega^2} \qquad 2.22$$

For **WTSB** the expression for $\tau_{G0}(\omega)$ remains the same, while

$$\tau_{G1}(\omega) = \frac{a_1}{\omega^2 + a_1^2} + \frac{\omega_1}{\omega^2 + \omega_1^2} + 2\omega_1 \sum_{k=2}^{3} \frac{h_k(\omega^2 + \omega_1^2)}{(\omega^2 - \omega_1^2)^2 + 4h_k^2\omega_1^2\omega^2} \qquad 2.23$$

The group delay for the three stations is shown in figure *2.8*. The low frequency part of the group delay is dominated by the seismometer, while the high frequency part is dominated by the anti-alias filter in combination with the GTS-1 high frequency cut-off. For frequencies lower than the corner frequency ω_1, the group delay shows a constant value, which can be estimated by:

$\tau_{G1}(\omega) = \dfrac{1 + 2\sum_{k=1}^{3} h_k}{\omega_1}$ for **HGN** and **WIT** and $\tau_{G1}(\omega) = \dfrac{1}{a_1} + \dfrac{1 + 2\sum_{k=2}^{3} h_k}{\omega_1}$ for **WTSB**.

Using these approximations, it becomes clear that an increase in corner frequency ω_1 between **HGN** and **WIT** of a factor 2 implies a reduction in group delay of a factor 2.

2.1.5 *Sensitivity*

The total system, as shown in figure 2.2, has a sensitivity:

$$S = S_{STS} \cdot 0.833 \cdot 256 \cdot (32768/20) = 3.49e+05 \cdot S_{STS}$$

where the factor 256 is the total gain for steps V5, V6 and V7 and the factor 32768/20 comes from the fact that the digitiser has 15 bit resolution and an input voltage of ±10 Volts. The sensitivity values should be multiplied by the normalisation constant a_0 , which is for the STS-1 equal to ω_1^7 and for the STS-2: $a_1\omega_1^5$. Please note that this definition of a normalisation constant is not the same as a normalisation constant in a SEED header, where a normalisation frequency is required.

Now the general features of the seismograph systems are given, the specific values for each station will be described in section 2.2-2.5.

2.1.6 *Timing*

For the timing of station **HGN, WIT** and **WTSB** a DCF-77 receiver is used. Time is added at the station site, before the data are sent over the telephone line to the central site in de Bilt. Status information on the time synchronisation is available in the data streams.

For station **OPLO** and the new generation of Quanterra based dataloggers, the timing system is replaced by a GPS system. No detailed study has been conducted yet to evaluate the accuracy of the different timing systems, although we assume an accuracy of 5-10 msec. This assumption is based on experience with the timing of the borehole systems (see chapter 3.8).

2.2 *Station HGN*

The sensors used at this station and their parameters are:

Sensor	S_{STS} [Vs/m]	Sensitivity (S)	Norm. const.	Sample rate
STS-1V (Z-comp) S/N 119001	2332	8.143E08	3.87E12	40 Hz
STS-1H (N-comp) S/N 29234	2314	8.080E08	3.87E12	40 Hz
STS-1H (E-comp) S/N 29235	2294	8.011E08	3.87E12	40 Hz

Moving over to a Quanterra datalogger in a test set-up with an STS-2 (3rd generation) in parallel with the old configuration gives a sensitivity: S= S_{STS} A cal[Z,N,E], where cal[Z]= 407468, cal[N]=415155 and cal[E]= 408655 all in [Counts/V], and A is the normalisation factor in equation ***1.4.3***:

Sensor	S_{STS} [Vs/m]	Sensitivity (S)
STS-2 (Z-comp)	1500	2.13E25
STS-2 (N-comp)	1500	2.17E25
STS-2 (E-comp)	1500	2.14E25

After the testing period the original STS-1 sensor will be coupled to the Quanterra datalogger, resulting in a sensitivity:

Sensor	S_{STS} [Vs/m]	Sensitivity (S)
STS-1 (Z-comp)	2332	3.75E12
STS-1 (N-comp)	2314	3.79E12
STS-1 (E-comp)	2294	3.70E12

2.3 *Station WIT*

The sensors used at this station are:

Sensor	S_{STS} [Vs/m]	Sensitivity (S)	Norm. const.	Sample rate
STS-1V (Z-comp) S/N 78417	2382	8.313E08	3.02E10	20 Hz
STS-1H (N-comp) S/N 78012	2180	7.608E08	3.02E10	20 Hz
STS-1H (E-comp) S/N 78013	2194	7.657E08	3.02E10	20 Hz

Sampling went up to 40 Hz with the change to a Quanterra data logger (see **2.6**)

S= S_{sts}cal[Z,N,E], where cal[Z]= 411457, cal[N]=409570 and cal[E]= 406487 all in [Counts/V], so:

Sensor	S_{STS} [Vs/m]	Sensitivity (S)
STS-1 (Z-comp)	2382	9.80E08
STS-1 (N-comp)	2180	8.93E08
STS-1 (E-comp)	2194	8.92E08

2.4 *Station WTSB*

Although the sensor is different, the same electronics has been used as for HGN. Therefore, the anti-alias filter has a 2-order less fall-off and the compensation pole is also not necessary. The STS-2 sensor has a serial number 119505 and is of the 2nd generation.

STS-2 (Z,N,E) $S_{STS-2} = 1500\,[Vs/m]$ S=5.24E08 Norm. Const.=4.17E10 40 sps

Recommendation:
Since the compensation pole is only useful in combination with an STS-1 sensor, it is recommended to remove this pole from the electronics scheme

2.5 *Station OPLO*

The sensor is an STS-2 (serial nr 29437) and is of the 1st generation, while the electronics only consists of a 24 bit digitizer and a FIR filter for anti-aliasing filter (Quanterra 4120). The FIR filter is characterized by a sharp cut-off in amplitude at 70-90% of the Nyquist frequency and a small effect on the phase that can be neglected in most cases (Hutt, 1993). A description of the FIR filters will be given in a separate publication by Sleeman (in prep.). Recording is in a 20 Hz continuous mode (BH) and 100 Hz triggered mode (HH).

S= S_{sts}cal[Z,N,E], where cal[1]= 406425, cal[2]=400350 and cal[3]= 424325 all in [Counts/V], so

Sensor	S_{STS} $[Vs/m]$	Sensitivity (S)
STS-2 (Z-comp)	1500	6.1E08
STS-2 (N-comp)	1500	6.0E08
STS-2 (E-comp)	1500	6.4E08

All information is now assembled to compare responses of the four broad-band stations in figure 2.6-2.8.

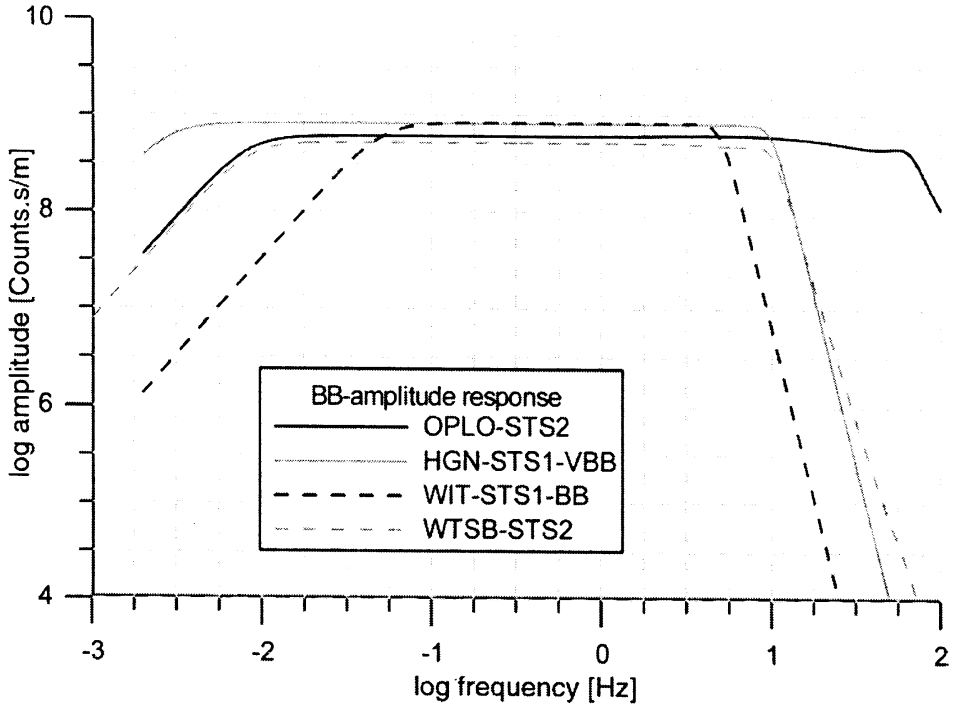

Figure 2.6. Amplitude response for ground velocity for four broad-band stations: ***HGN, WIT, WTSB*** *and* ***OPLO.*** *For* ***OPLO*** *the FIR filter effects are not shown.*

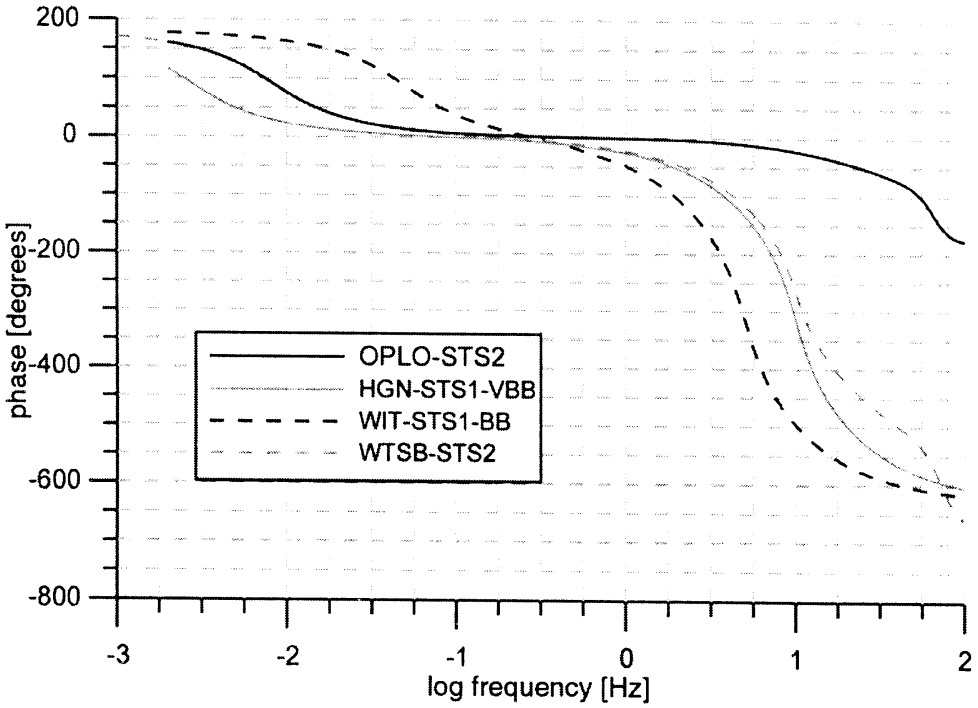

Figure 2.7. Phase response for ground velocity for four broad-band stations: ***HGN, WIT, WTSB*** *and* ***OPLO.*** *For* ***OPLO*** *the FIR filter effects are not shown.*

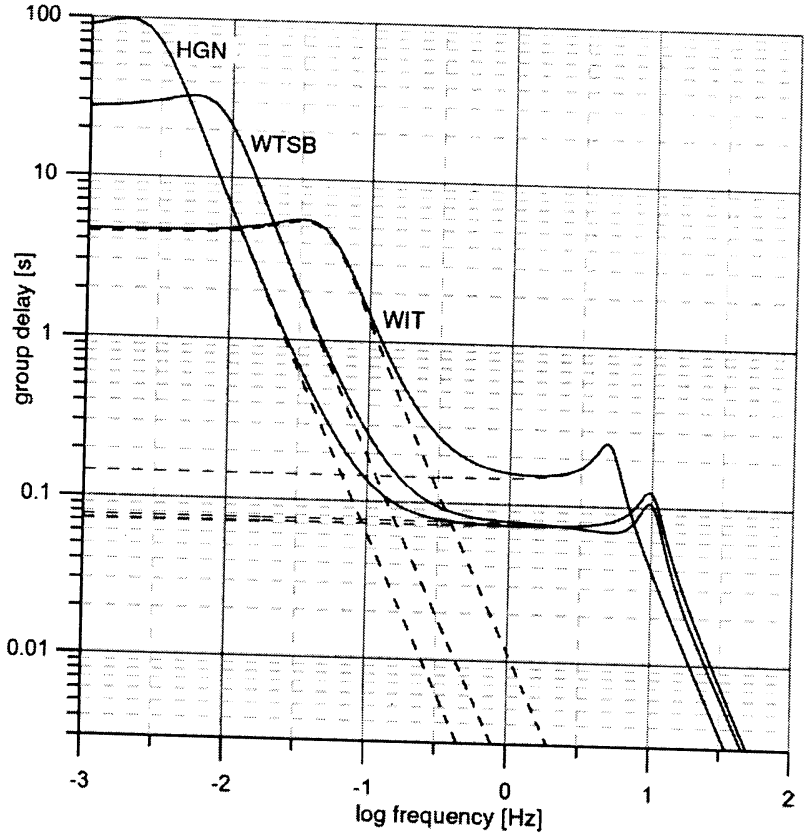

Figure 2.8. Group delay as a function of frequency for station ***HGN, WIT*** *and* ***WTSB***

2.6 Modification history and developments

Station **HGN** did change its sampling rate from 20 Hz to 40 Hz at November 3, 1993 (13:00 hrs). This modification of the original electronics was necessary, since it was based on the BB sensor instead of the VBB sensor. No further modifications in the electronics were made. For station **WTSB** the N and E components were interchanged and restored on June 8, 2000. Station **OPLO** is operational with a Quanterra 4120 data logger and is operated with a data repository on an internal ring buffer. The station is accessible by a modem connection. Initially the STS-2 in **OPLO** was positioned with the N component pointing in the E direction and the E direction pointing to the South. This was repaired March 23, 2000.

The time of operation of the broad-band stations are:

Station name	Operational since	Sampling rate	Date of changes
HGN	February 23, 1993	20 → 40 Hz	November 3, 1993
WIT	November 16, 1993	20 → 40 Hz	December 13, 2000
OPLO	September 7, 1998	20 Hz + 100 Hz	March 23, 2000
WTSB	February 21, 2000	40 Hz	June 8, 2000

For all broad-band stations operating with the 'Graefenberg'-type hardware, digital data acquisition will be upgraded to a 24 bits Quanterra data logger. This implies that all anti-alias filters (except for the 2nd order filters from the STS-1 itself) are replaced by a set of FIR filters. For **HGN, WIT** and **WTSB** the Quanterra system should operate in a real-time data transmission mode. Station **WIT** is operating with the Quanterra data logger and a sampling rate of 40 Hz in an experimental mode since December 13, 2000. In 2002 it is expected that stations **HGN** and **WTSB** will also be upgraded to 24 bits recording like **WIT**.

At **HGN** an experimental system runs in parallel with the 'old' instrumentation. This system consists of an STS-2 (S/N 110015, 3rd generation) and a Quanterra (4126GD-2/E8) datalogger. This experimental set up started to operate 6/6/2001.

The next two figures show the amplitude and phase response of the new Quanterra systems running in **HGN** and **WIT.**

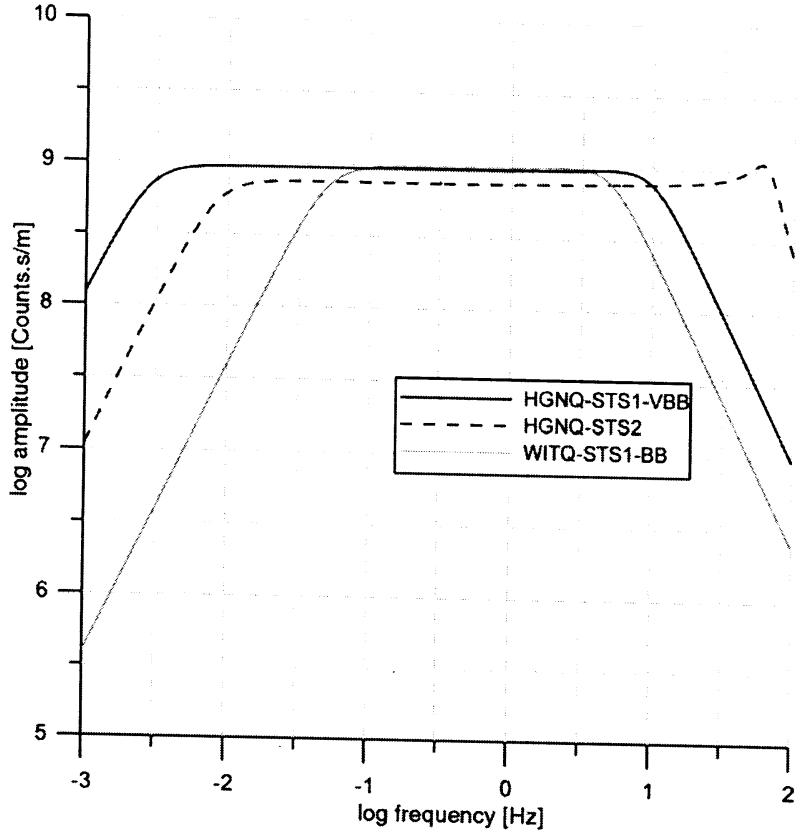

Figure 2.9: Amplitude response of the new Quanterra systems, without FIR filters

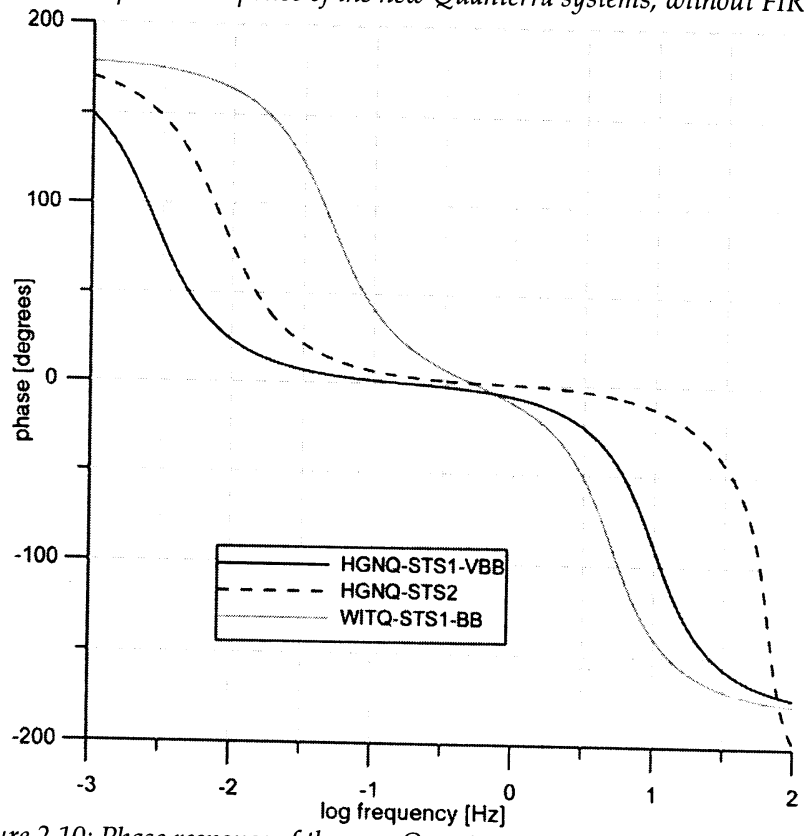

Figure 2.10: Phase response of the new Quanterra systems, without FIR filters

2.7 *Summary of response information*

The following table gives an overview of the response information of the broad-band systems for the stations that have been described in this section. The response has a general form:

$$T_{tot}(s) = \frac{S\prod_{i=1}^{k}(s - z_i)}{\prod_{j=1}^{l}(s - s_j)} \qquad 2.21$$

	HGN	WIT	WTSB	OPLO-Q
S	3.15E21 (Z) 3.13E21 (N) 3.10E21 (E)	2.51E19 (Z) 2.30E19 (N) 2.31E19 (E)	1.03E37 (Z,N,E)	3.51E21 (Z) 3.45E21 (N) 3.68E21 (E)
np	9	9	20	9
s_1	(-0.01234, 0.01234)	(-0.222, 0.222)	(-0.037, 0.037)	(-0.037, 0.037)
s_2	(-0.01234, -0.01234)	(-0.222, -0.222)	(-0.037, -0.037)	(-0.037, -0.037)
s_3	(-62.832, 0.00)	(-31.416, 0.00)	(-62.832, 0.00)	(-7454.,7142)
s_4	(-39.144, 49.148)	(-19.572, 24.574)	(-56.612, 27.258)	(-7454.,-7142)
s_5	(-39.144, -49.148)	(-19.572, -24.574)	(-56.612, -27.258)	(-417.1, 0.00)
s_6	(-56.612, 27.258)	(-28.306, 13.629)	(-14.012, 61.250)	(-100.9, 401.9)
s_7	(-56.612, -27.258)	(-28.306, -13.629)	(-14.012, -61.250)	(-100.9, -401.9)
s_8	(-14.012, 61.250)	(-7.006, 30.625)	(-85.11 0.00)	(-15.99, 0.00)
s_9	(-14.012, -61.250)	(-7.006, -30.625)	(-6909, -9208)	(-187.24, 0.00)
s_{10}			(-6909, 9208)	
s_{11}			(-6227, 0.0)	
s_{12}			(-4936, -4713)	
s_{13}			(-4936, 4713)	
s_{14}			(-1391, 0.0)	
s_{15}			(-556.8, -60.05)	
s_{16}			(-556.8, 60.05	
s_{17}			(-98.44, -442.8)	
s_{18}			(-98.44, -442.8)	
s_{19}			(-10.95, 0.00)	
s_{20}			(-255.1, 0.00)	
nz	3	3	10	6
z_1	(0.00, 0.00)	(0.00, 0.00)	(0.00, 0.00)	(0.00, 0.00)
z_2	(0.00, 0.00)	(0.00, 0.00)	(0.00, 0.00)	(0.00, 0.00)
z_3	(0.00, 0.00)	(0.00, 0.00)	(0.00, 0.00)	(0.00, 0.00)
z_4			(-5907., 3411.)	(-318.6, 401.2)
z_5			(-5907., -3411.)	(-318.6, -401.2)
z_6			(-683.9, 175.5)	(-15.15, 0.00)
z_7			(-683.9, -175.5)	
z_8			(-555.1, 0.00)	
z_9			(-294.6, 0.00)	
z_{10}			(-10.75, 0.00)	

New systems:

	HGN-Q (STS2)	HGN-Q (STS1-VBB)	WIT-Q (STS1-BB)
S	2.13E25 (Z) 2.17E25 (N) 2.14E25 (E)	3.75E12 (Z) 3.79E12 (N) 3.70E12 (E)	9.67E11 (V) 8.81E11 (N) 8.80E11 (E)
np	11	4	4
s_1	(-0.037, 0.037)	(-0.01234, 0.01234)	(-0.222, 0.222)
s_2	(-0.037, 0.037)	(-0.01234, -0.01234)	(-0.222, -0.222)
s_3	(-13300, 0.0)	(-39.144, 49.148)	(-19.572, 24.574)
s_4	(-10530, -10050)	(-39.144, -49.148)	(-19.572, -24.574)
s_5	(-10530, 10050)		
s_6	(-520.3, 0.0)		
s_7	(-374.8, 0.0)		
s_8	(-97.34, -400.7)		
s_9	(-97.34, 400.7)		
s_{10}	(-15.64, 0.0)		
s_{11}	(-255.1, 0.00)		
nz	7	3	3
z_1	(0.00, 0.00)	(0.00, 0.00)	(0.00, 0.00)
z_2	(0.00, 0.00)	(0.00, 0.00)	(0.00, 0.00)
z_3	(0.00, 0.00)	(0.00, 0.00)	(0.00, 0.00)
z_4	(-461.8, 429.1)		
z_5	(-461.8, -429.1)		
z_6	(-220.,0.00)		
z_7	(-15.15, 0.00)		

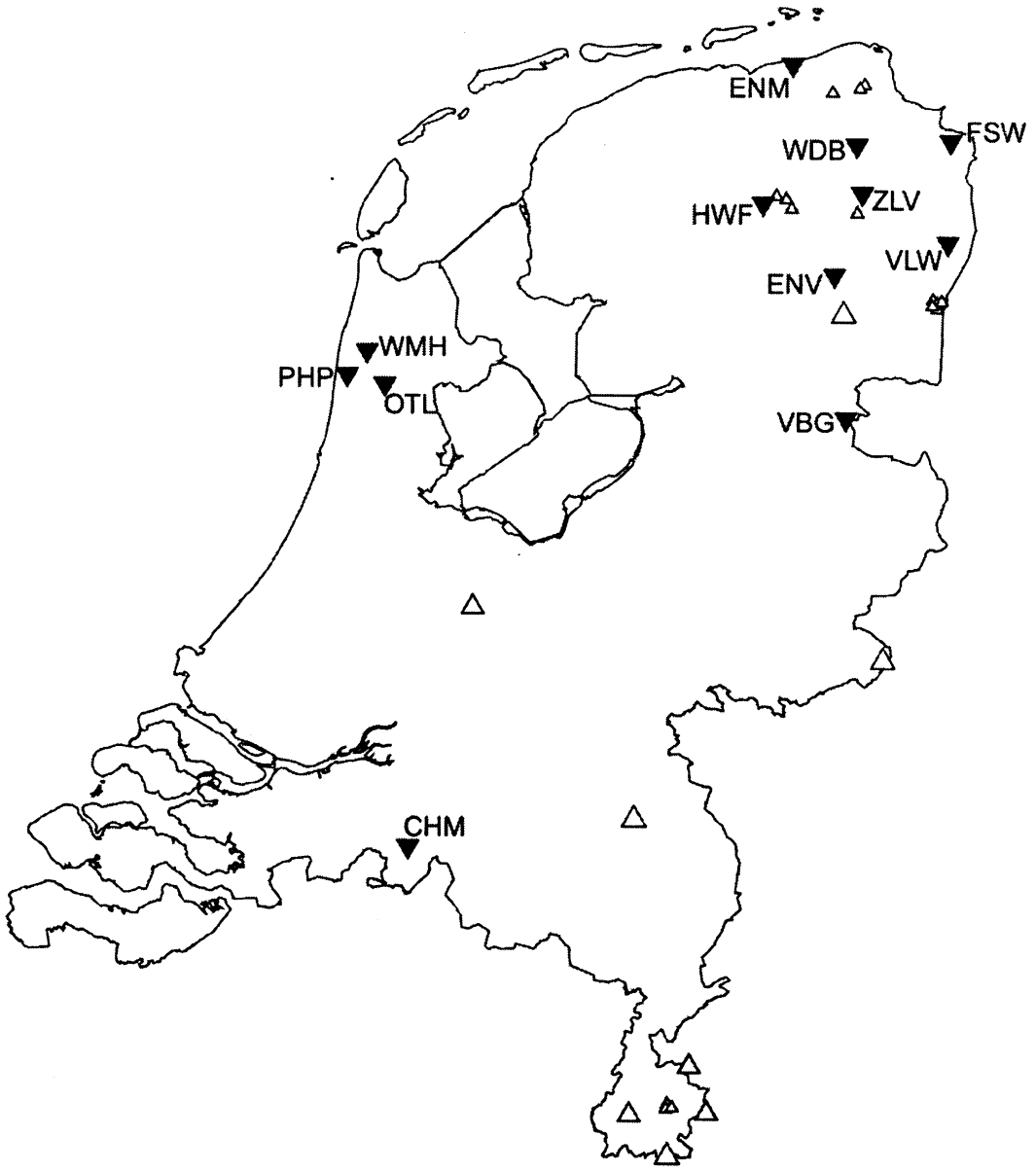

Figure 3.1. Overview of seismic stations in the Netherlands, installed and maintained by the KNMI (status: summer 2002). Short period borehole stations are shown as filled inverted triangles.

3. Short period borehole instrumentation

A borehole seismograph, as deployed by the KNMI, consists of a string with 4 (or 5 in case of **FSW**) levels of 3 component geophones. The geophones are SM6 instruments and are characterized by a corner frequency of 4.5 Hz. Although one station (**FSW**) did operate at this corner frequency from 1991 to 1995, a design requirement became an enlarged pass-band (down to 1.0 Hz). For this purpose a correction filter was designed. A high pass filter at 0.15 Hz was added for stability. Finally, an 8-order Butterworth filter was applied as anti-aliasing filter with a corner frequency at 28 Hz.

3.1 Sensor

The transfer function of the geophone for displacement is given by

$$T_s(s) = \frac{s^3 S}{s^2 + 2h_0\omega_0 s + \omega_0{}^2} \qquad 3.1$$

where $\omega_0 = 2\pi\ 4.5 = 28.27$ rad/s. The damping parameter h_0 is dependent on the value of the shunt resistor . According to the specifications a shunt resistance of 8200 Ω is needed to give a damping of 0.707, so

$$T_s(s) = \frac{s^3 S}{(s - s_1)(s - s_1^*)}, \text{ with } s_1=(-19.99, 19.99) \text{ and } S= 28.8 \text{ V/m}$$

3.2 Correction filter

After the amplification, a correction filter (S-shaped filter) is applied in order to move the corner frequency of the seismometer from 4.5 Hz to 1 Hz.

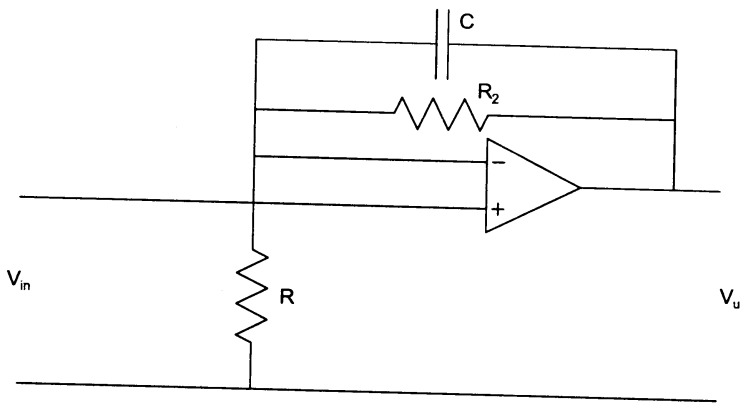

Figure 3.2. Electronics scheme for one stage of the correction filter

Two identical stages are implemented, shown in figure 3.2. For each stage, the equations are:

$$(V_u - V_i)(\frac{1}{R_2} + sC) = V_i \cdot \frac{1}{R} \qquad 3.2$$

$$T(s) = \frac{(\frac{1}{RC} + \frac{1}{R_2C}) + s}{\frac{1}{R_2C} + s} = \frac{(s+\omega_0)}{(s+\omega_1)} \qquad 3.3$$

and

$$T_{hp}(s) = \frac{(s+\omega_0)^2}{(s+\omega_1)^2} \qquad 3.4$$

Selection of components:
R = 3010 Ω, R_2 = 10600 Ω and C= 15 μF.

Then ω_0 = 28.44 rad/s (or f_0= 4.5 Hz) and ω_1 = 6.29 rad/s (or f_1= 1.0 Hz) and the pole and zero values are:

s_2 = (-28.44, 0.00)
s_3 = (-6.29, 0.00)

Unfortunately, the zero value doe not compensate the pole of the seismometer exactly. A more general description of possible correction filters is given by Dost et al., 1984 and is treated in section **3.2.1**.

Application to 10 Hz geophones:

This filter could also be applied to geophones operating at higher eigenfrequencies. An example is a VSP-string near Chaam (CHM), which is abandoned by Shell and made available as "borehole-string" to the KNMI. The geophones are similar to the 4.5 Hz geophones in the other borehole installations, except for the eigenfrequency at 10 Hz. If the same value for C and R_2 are used as in the 4.5 Hz case, then the resulting value for R= 1178 Ω. This value is low compared to R_2 and may introduce a large DC offset (dependent on the ratio between the resistances). From equation **3.3** one can write:

$$\omega_0 = \frac{1}{RC} + \frac{1}{R_2C}\ ,\ \omega_1 = \frac{1}{R_2C}\ ,\ \text{so}\ \ R = \frac{1}{(\omega_0 - \omega_1)C}\ \text{and}\ R_2 = \frac{1}{\omega_1 C} \qquad 3.5$$

The ratio between the resistances is independent from the value of C. Since the value for ω_0 is determined by the sensor, the only freedom is to change the value of ω_1 to higher values. An increase in the value for C does require lower values for both resistances, which reduces the noise.

3.2.1 *General description of the correction filter*

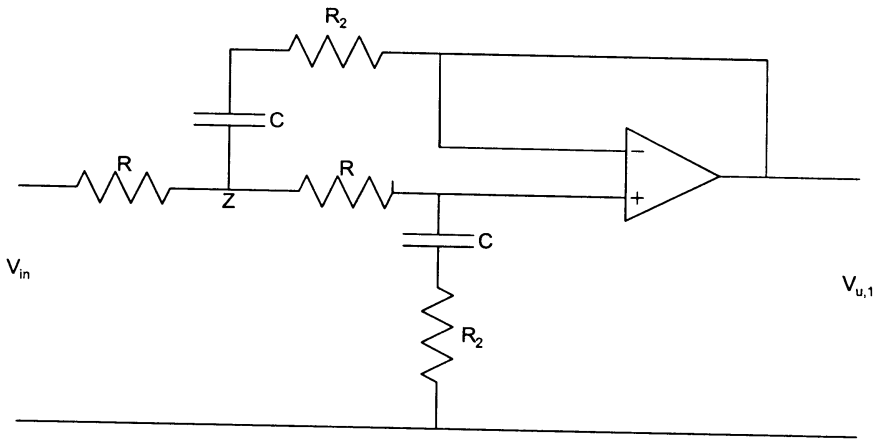

Figure 3.3. Electronics scheme for a more general correction filter

An alternative correction filter is shown in figure *3.3*. For a more efficient calculation, we use admittances in the calculations. So, if the admittances are:

$Y_1 = \frac{1}{R}$, $Y_2 = \frac{1}{R}$, $Y_3 = (\frac{1}{Cs} + R_2)^{-1} = \frac{Cs}{1 + R_2 Cs}$ and $Y_4 = Y_3$, the equations become an extension of *2.12* and *2.13*:

$$(V_{in} - V_z)Y_1 + (V_u - V_z)Y_2 - (V_z - V_u)Y_3 = 0 \qquad 3.6$$

$$(V_u - V_z)Y_2 + V_u Y_4 = 0 \qquad 3.7$$

From equation *3.7* follows: $V_z = \frac{Y_2 + Y_4}{Y_2} V_u$ and substitution in *3.6* gives:

$$\frac{U_u}{V_{in}} = \frac{Y_1 Y_2}{Y_1 Y_2 + Y_4(Y_1 + Y_2 + Y_3)} = \frac{(1 + R_2 Cs)(1 + R_2 Cs)}{(1 + R_2 Cs)(1 + R_2 Cs) + Cs[..]} = \frac{\omega_1^{\,2}}{\omega_0^{\,2}} \cdot \frac{(s^2 + 2h_0\omega_0 s + \omega_0^{\,2})}{(s^2 + 2h_1\omega_1 s + \omega_1^{\,2})} \qquad 3.8$$

If the numerator is required to have the form $\frac{1}{\omega_0^{\,2}} \cdot (s^2 + 2h_0\omega_0 s + \omega_0^{\,2})$, a requirement for real values for the factor h_0 gives: h_0 =1.0. Even if equation *3.8* is generalised and all R and C values are assumed independent, still the requirement is h_0 >= 1.0. Therefore, the alternative is equal to the original formulation and therefore shows no improvement. The only difference between equations *3.4* and *3.8* is a factor $\frac{\omega_1^{\,2}}{\omega_0^{\,2}}$ in the last equation, that could be compensated by an additional amplification stage.

The damping of the sensor could be increased by decreasing the value of the shunt resistor of 8200Ω. According to the manual, a shunt resistance of 3300Ω already increases the damping from a value of 0.71 to a value of 0.91. However, this influences the response of the sensor to the lower frequencies against the design criteria.

3.3 *High-pass filter*

At the borehole instrumentation, a high-pass filter is included in order to suppress low frequency noise. The electronics scheme is shown in figure 3.4.

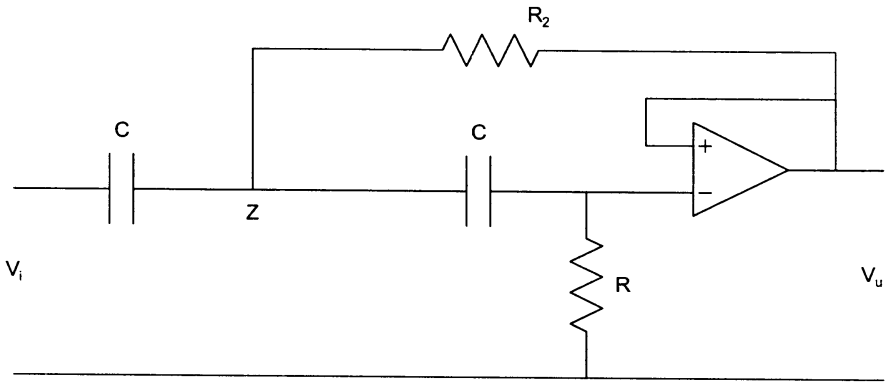

Figure 3.4: Electronics scheme for the high pass filter

The transfer function can be calculated:

$$(V_i - V_z)sC + (V_u - V_z)\cdot\frac{1}{R_2} - (V_z - V_u)sC = 0 \qquad 3.9$$

$$(V_z - V_u)sC = V_u \cdot \frac{1}{R} \qquad 3.10$$

The term V_z can be expressed into V_u by reworking the last equation:

$$V_z = \frac{1+sCR}{sCR}\cdot V_u \qquad 3.11$$

Substitution in equation 3.6 leads to:

$$V_u[\frac{1+sCR_2}{R_2} - \frac{1+sCR}{sCR}\cdot\frac{1+2sCR_2}{R_2}] = -sCV_i \qquad 3.12$$

and

$$\frac{V_u}{V_i} = \frac{-s^2C^2RR_2}{-s^2C^2RR_2 - 2sCR_2 - 1} = \frac{s^2}{s^2 + 2\omega_2 h_2 s + \omega_2{}^2} = \frac{s^2}{(s-s_4)(s-s_4^*)} \qquad 3.13$$

where $\omega_2{}^2 = \frac{1}{C^2RR_2}$ and $h_2{}^2 = \frac{R_2}{R}$

The components used in the electronics are:

$C = 15\ \mu\text{F}$, $R = 100\cdot10^3\ \Omega$ and $R_2 = 47.5\cdot10^3\ \Omega$

resulting in a value for $\omega_2 = 0.967$ rad/s (or a cut-of frequency of 0.15Hz) and $h_2 = 0.689$,so

s_4 = (-0.666, 0.701)

3.4 *Anti-aliasing filter*

The equations for an 8th order Butterworth filter are:

$$T_{al}(s) = \frac{\omega_3^{\,2}}{s^2 + 0.390\omega_3 s + \omega_3^{\,2}} \cdot \frac{\omega_3^{\,2}}{s^2 + 1.111\omega_3 s + \omega_3^{\,2}} \cdot \frac{\omega_3^{\,2}}{s^2 + 1.663\omega_3 s + \omega_3^{\,2}} \cdot \frac{\omega_3^{\,2}}{s^2 + 1.962\omega_3 s + \omega_3^{\,2}} \qquad 3.14$$

with $\omega_3 = 2\pi\ 28 = 175.9$ rad/s; the poles are:

s_5 = (-34.30, -172.52)
s_6 = (-97.71, -146.26)
s_7 = (-146.26, -97.72)
s_8 = (-172.56, -34.13)

3.5 *Total transfer function*

$$T_{tot}(s) = T_{geoph}(s) \cdot T_{cor}(s) \cdot T_{hp}(s) \cdot T_{al}(s)$$

$$T_{tot}(s) = \frac{Ss^3}{(s^2 + 2h_0\omega_0 s + \omega_0^{\,2})} \cdot \frac{(s+\omega_0)^2}{(s+\omega_1)^2} \cdot \frac{s^2}{(s^2 + 2h_2\omega_2 s + \omega_2^{\,2})} \cdot \prod_{k=3}^{6} \frac{\omega_3^{\,2}}{s^2 + 2h_k\omega_3 s + \omega_3^{\,2}} \qquad 3.15$$

$$T_{tot}(s) = \frac{Ss^3}{(s-s_1)(s-s_1^{\,*})} \cdot \frac{(s-s_2)^2}{(s-s_3)^2} \cdot \frac{s^2}{(s-s_4)(s-s_4^{\,*})} \cdot \prod_{k=3}^{6} \frac{\omega_3^{\,2}}{(s-s_{k+2})(s-s_{k+2}^{\,*})}$$

With

s_1 = (-19.99, 19.99)
s_2 = (-28.50, 00.00)
s_3 = (-6.35, 00.00)
s_4 = (-0.666, 0.701)
s_5 = (-34.30, -172.52)
s_6 = (-97.71, -146.26)
s_7 = (-146.26, -97.72)
s_8 = (-172.56, -34.13)

3.6 Sensitivity

Old system

Electronic amplification is a factor 1000, after a first amplification factor of 0.956 (8200/(8200+375)). The old 12 bits AD board (Data Translation DT-2824 PGH) is used at a gain setting of 4, meaning an amplification of a factor 100. The A/D board has a maximum of 4096 Counts at 20V input difference. Therefore the sensitivity is:

$$S = 28.8 \cdot 1000 \cdot 0.956 \cdot 100 \cdot 4096 / 20.[Counts \cdot s / m] = 5.64e + 08[Counts \cdot s / m]$$

New System

The main difference in sensitivity with respect to the old system is the use of a 16 bit A/D converter (PC-LabCard PCL-816, Advantech Corp.), where a maximum of 65536 Counts are used for a maximum input difference of 20 Volts. Also, the additional amplification of a factor 100 could be left out. Different gain factors can be applied in the application software (HDETECT). These settings are defined as follows:

Gain number	factor
3	8
2	4
1	2
0	1

All the borehole stations are configured with a gain setting 2, which implies a gain factor of 4, so:

$$S = 28.8 \cdot 1000 \cdot 0.956 \cdot 65536 / 20.[Counts \cdot s / m] = 3.61e + 08[Counts \cdot s / m]$$

3.7 Modification history and developments

Station **FSW** did operate in the original set-up (without correction filter and with 12 bits recording) from July 7, 1992 until May 5, 1996. Since then the station is compatible to the other 10 borehole stations in the Northern part of the Netherlands. The sampling rate of the borehole instruments is 120 Hz. Data is available in continuous data streams in a ring buffer that lasts for app. 3 days.

3.8 Timing

Timing of the borehole systems is realised using a DCF-77 receiver. The DCF signal is recorded digitally as a separate data channel. Evaluation of the timing history shows that on average a timing error less than 5 msec is achieved.

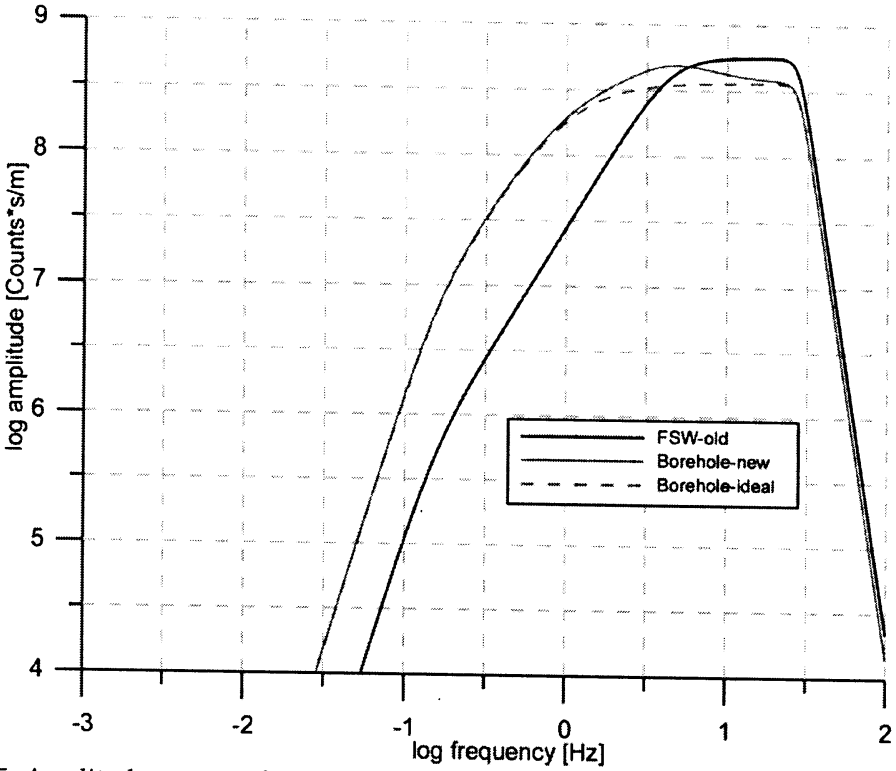

Figure 3.5: Amplitude response for the borehole system. Indicated are the responses of the original (old) response, the intended design response and the realised response.

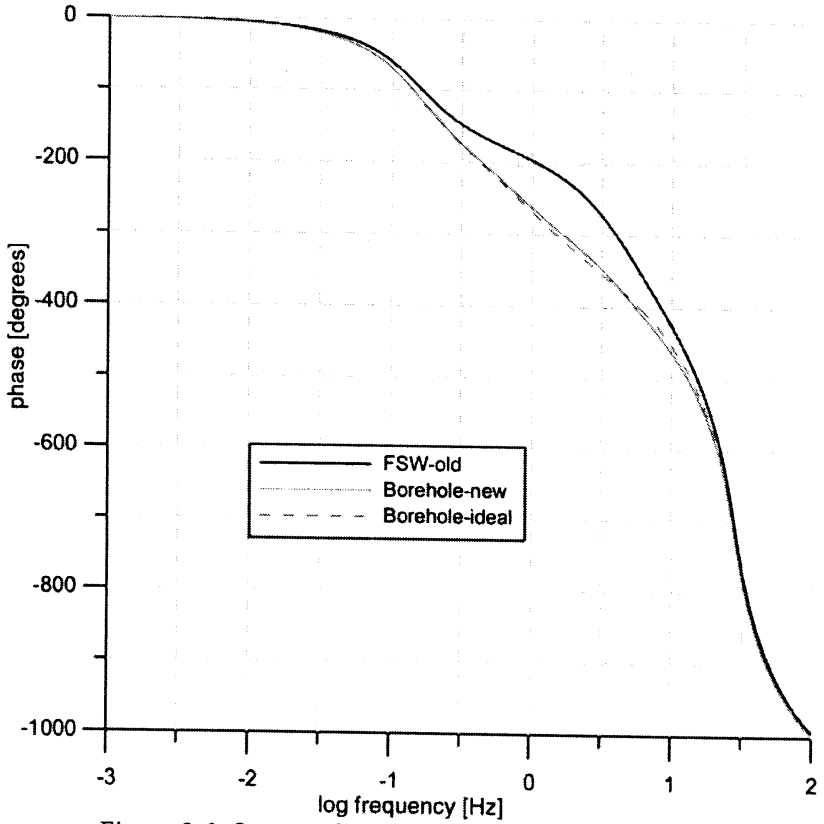

Figure 3.6: Same as figure 3.5, but now phase response

3.9 Summary of response information

The following table gives an overview of the response information of the borehole systems for the stations that have been described in this section. The response has a general form:

$$T_{tot}(s) = \frac{S\prod_{i=1}^{k}(s - z_i)}{\prod_{j=1}^{l}(s - s_j)}$$

	FSW-old	**Borehole_new**	**Borehole_ideal**
S	5.17E26	3.31E26	3.31E26
np	12	14	12
s_1	(-19.99, 19.99)	(-19.99, 19.99)	(-6.35, 0.00)
s_2	(-19.99, -19.99)	(-19.99, -19.99)	(-6.35, 0.00)
s_3	(-0.666, 0.701)	(-6.35, 0.00)	(-0.666, 0.701)
s_4	(-0.666, -0.701)	(-6.35, 0.00)	(-0.666, -0.701)
s_5	(-34.30, 172.52)	(-0.666, 0.701)	(-34.30, 172.52)
s_6	(-34.30, -172.52)	(-0.666, -0.701)	(-34.30, -172.52)
s_7	(-97.71, 146.26)	(-34.30, 172.52)	(-97.71, 146.26)
s_8	(-97.71, -146.26)	(-34.30, -172.52)	(-97.71, -146.26)
s_9	(-146.26, 97.72)	(-97.71, 146.26)	(-146.26, 97.72)
s_{10}	(-146.26, -97.72)	(-97.71, -146.26)	(-146.26, -97.72)
s_{11}	(-172.56, 34.13)	(-146.26, 97.72)	(-172.56, 34.13)
s_{12}	(-172.56, -34.13)	(-146.26, -97.72)	(-172.56, -34.13)
s_{13}		(-172.56, 34.13)	
s_{14}		(-172.56, -34.13)	
nz	5	7	5
z_1	(0.00, 0.00)	(0.00, 0.00)	(0.00, 0.00)
z_2	(0.00, 0.00)	(0.00, 0.00)	(0.00, 0.00)
z_3	(0.00, 0.00)	(0.00, 0.00)	(0.00, 0.00)
z_4	(0.00, 0.00)	(0.00, 0.00)	(0.00, 0.00)
z_5	(0.00, 0.00)	(0.00, 0.00)	(0.00, 0.00)
z_6		(-28.50, 0.00)	
z_7		(-28.50, 0.00)	

Figure 4.1. Overview of seismic stations in the Netherlands, installed and maintained by the KNMI (status: summer 2002). Short period surface stations are shown as filled triangles.

4. Short period surface instrumentation

In addition to the broad-band stations in the southern part of the Netherlands, four short period stations (**VKB, RDC, SCHN, HGN**) are added, all equipped with three Willmore MkIIIA sensors. For **HGN** this means a co-location of a broad-band and short-period sensor. The electronics is similar to the electronics of the (16-bit) borehole systems, without the correction filter. The same set-up, with a Willmore Mk II or Mk IIIA sensor (Z-component only), was used in short period stations in the northern part of the Netherlands that existed prior to the development of the short period borehole stations and the broad-band stations. The stations are: the **Assen array, WIT** and **WTS**. In the southern part of the Netherlands stations **HEE, KRN** and **ENN** are also operated with a vertical component only. The first two stations (**HEE** and **KRN**) were operational in the 70's and 80's. Their response is uncertain and the stations did not deliver much data, so in the present version of this document we will only specify some known characteristics.

4.1 Sensor

The Willmore seismometer has a transfer function of:

$$T_s(s) = \frac{s^3 S}{s^2 + 2h_0\omega_0 s + \omega_0^{\,2}} \qquad 4.1$$

where ω_0 = 6.28 rad/s (f_0 = 1Hz). Details for each station are specified in section 4.5. Two different kinds of Willmore sensors are used by the KNMI: the Mark II and the Mark IIIA, which will be described below.

Mark II:
This is the oldest sensor. The sensitivity of the main coil (R_c) of 3300 Ω is 570 Vs/m (see manual page B12). The damping is directly determined by the value of the external resistance used. This value is different for each station and ranges from 6800 Ω (**ENN**) to 10000 Ω (**WTS**). The damping D and eigen period of the sensor T are related through the equation:

$$\frac{R}{R_c} = n + 1 = 1.7\frac{T}{D} \qquad 4.2$$

Mark IIIA:
This sensor has a sensitivity between 490 and 550 Vs/m (average 520 Vs/m) and a coil resistance of $2 \cdot 8 - 2 \cdot 10\,\mathrm{k}\Omega$. Damping is determined by the external resistance used and can be calculated following the general formula as given by Aki and Richards (1980, p 508):

$$h_0 = \frac{\varepsilon}{\omega_0} = \frac{S^2}{2(R_c + R)M\omega_0} \qquad 4.3$$

where M is the mass of 1.2 kg.

4.2 *High pass and anti-aliasing filters*

The design of these filters is equal to the ones used in the borehole electronics. However, for station **HGN**-hh and **SCHN** a different value for the capacitors is used (see chapter 4.5). All stations of the Assen array and stations **ENN, WIT, HEE, KRN** and **WTS** did transmit their data using PCM modulation through the Motorola TM-205 board. This board is equipped with two stages of a 2-pole low-pass filter, which has a transfer function:

$$T_s(s) = \frac{\omega_0^2}{(s+\omega_0)^2} \cdot \frac{\omega_0^2}{(s+\omega_0)^2} \text{ , with } \omega_0 = 42.64 \text{ rad/s } (f_0 = 6.8 \text{ Hz})$$

4.3 *Total transfer function*

The description of the total response of the seismic stations differs in details concerning damping, gain and the use of high-pass or low-pass filters. All systems have in common the anti-alias filters that are described in the previous section, so in general:

$$T_{tot}(s) = T_s(s) \cdot T_{hp}(s) \cdot T_{lp}(s) \cdot T_{al}(s)$$

$$T_{tot}(s) = \frac{Ss^3}{(s-s_1)(s-s_1^*)} \cdot T_{hp}(s) \cdot T_{lp}(s) \cdot \prod_{k=3}^{6} \frac{\omega_3^2}{(s-s_k)(s-s_k^*)} \qquad 4.4$$

with

$\omega_3 = 175.9$ rad/s
$s_3 = (-34.30, -172.52)$
$s_4 = (-97.71, -146.26)$
$s_5 = (-146.26, -97.72)$
$s_6 = (-172.56, -34.13)$

In the following chapters the different systems will be described.

4.3.1 *The Assen array*

All six stations (**ZYN, WSB, RLD, LGV, BVS** and **MWD**) are equipped with a Willmore Mk IIIA sensor. The coil resistances are $2 \cdot 10\,\text{k}\Omega$ and the sensitivity is 520 Vs/m. The external load applied is $6.8\,\text{k}\Omega$, so the resulting damping is $h_0 = \frac{(520)^2}{2 \cdot (26800) \cdot 1.2 \cdot 2\pi} = 0.67$.
The electronics following the sensor include a one-pole low-pass filter at a corner frequency of 31.45 rad/s (5.0 Hz) and an amplification factor of 45. This filter is followed by a one pole high-pass filter at 0.67 rad/s (0.11 Hz). The signal is then fed into a Motorola TM 105 card and sent by telephone to the central site at the KNMI, where the signal is received by a Motorola TM 205 card. This last card contains additional low-pass filters described in section 4.2

Finally, the data are captured by a 12 bits A/D board and recorded in digital form.

The total transfer function becomes:

$$T_{tot}(s) = T_s(s) \cdot T_{lp}(s) \cdot T_{hp}(s) \cdot T_{205}(s) \cdot T_{al}(s)$$

$$T_{tot}(s) = \frac{Ss^3}{(s^2 + 2h_0\omega_0 s + \omega_0{}^2)} \cdot \frac{V\omega_1}{(s+\omega_1)} \cdot \frac{s}{(s+\omega_2)} \cdot \frac{\omega_3{}^4}{(s+\omega_3)^4} \cdot \prod_{k=5}^{8} \frac{\omega_4{}^2}{s^2 + 2h_k\omega_4 s + \omega_4{}^2} \qquad 4.5$$

$$T_{tot}(s) = \frac{Ss^3}{(s-s_1)(s-s_1^*)} \cdot \frac{V\omega_1}{(s-s_2)} \cdot \frac{s}{(s-s_3)} \cdot \frac{\omega_3{}^4}{(s-s_4)^4} \cdot \prod_{k=5}^{8} \frac{\omega_4{}^2}{(s-s_k)(s-s_k^*)}$$

s_1 = (-4.21, 4.65), S= 520 Vs/m V=45
s_2 = (-31.45, 0.0)
s_3 = (-0.67, 0.0)
s_4 = (-42.64, 0.00)

The other values of the poles of the anti-alias filter are the same as in section 4.3

4.3.2 *Stations WIT, WTS, ENN*

These stations are equipped with a Willmore Mark II sensor, vertical component only. The settings are described in the following table:

Station name	External load (Ω)	T (s)	D
WIT	10000	1.0	0.56
WTS	10000	1.0	0.56
ENN	6800	1.0	0.83

In all three stations the next stage in electronics is a first order low-pass filter. The values for the amplification and low-pass corner frequency for this stage are summarized in the following table:

Station name	amplification	ω_0 [rad/s]	Frequency [Hz]
WIT	82	16.84	2.7
WTS	150	13.78	2.2
ENN	383	16.84	2.7

Before going into the Motorola 205 card, station ENN has an additional one pole low-pass filter at a corner frequency of 200 rad/s (31.83 Hz) and an additional gain of 1.4.

In addition data acquisition is arranged through the use of a 12 bit A/D board, similar to the one described in section 3.6.

4.3.3 *Stations VKB, RDC, SCHN, HGN (HEE, KRN)*

These stations are equipped with a set of three Willmore Mk-IIIA sensors (Z,NS,EW).

4.4 Sensitivity

The seismic stations can be separated into two groups:

Assen array, station ***WIT, WTS, ENN (KRN, HEE)***

The total sensitivity of these station is different for each station, but for the A/D sensitivity is:

$$T \cdot 4096/20 \text{ [Counts/V]} = T \cdot 204.8 \text{ [Counts/V]},$$

where T is the gain setting at the A/D board (Data Translation DT 2824 PGL) and is user selectable through an input file. These settings change over time. Data from these stations come together in one file using the IASPEI mdetect software. Different settings can be recognized from the station naming and we can reconstruct these settings:

Assen stations, **WIT,WTS,ENN,KRN,VKB,WOOF,ENN,VKB,FINS (ENN** 2 times)
All stations have a T=8, except for **WIT** (T=4)
Assen stations, **WIT,WTS,ENN,KRN,VKB,WOOF,TRIG,TRIG,TRIG**
All stations have a T=4
Assen stations, **WITz,WTSz,ENNz, HEEz, VKBz, WOOF,ENN2,VKB2,FINS**
All stations have a T=8, except for **WITz** and HRLz (T=4)
VKBn,VKBe, VKBz,LOOS,LOOS,HGN,WITz,WTSZ,ENNz,HEEz,VKBz,WOOF, ENN2,LOOS,FI5Z.
All stations have a T=8, except **HGN, WITz** (both T=4)
ZYNz, RLDz,BVSz,WSBz, WSBn,WSBe,WITz, WTSz,ENNz,HEEz,VKBz,WOOF,..
All stations have T=8, except **WITz** and **HEEz** (both T=4)

Normalisation of the total response equation for the **Assen** array gives a factor:
$31.45 \cdot (42.64)^4 \cdot (175.9)^8 = 9.53E25$. So, the total sensitivity for the **Assen** array is:

$$S = 520 \cdot 0.254 \cdot 45 \cdot 8 \cdot 204.8 \cdot 9.53E25 = \textbf{9.28E32} \text{ [Counts.s/m]}$$

For station **WIT**, the normalisation factor is: $16.84 \cdot (42.64)^4 \cdot (175.9)^8 = 5.10E25$
So, total sensitivity for station **WIT** is:

$$S = 570 \cdot 82 \cdot 4 \cdot 204.8 \cdot 5.10E25 = \textbf{1.95E33} \text{ [Counts.s/m]}$$

For station **WTS**, the normalisation factor is: $13.78 \cdot (42.64)^4 \cdot (175.9)^8 = 4.17E25$
So, total sensitivity for station **WTS** is:

$$S = 570 \cdot 150 \cdot 8 \cdot 204.8 \cdot 4.17E25 = \textbf{5.84E33} \text{ [Counts.s/m]}$$

For station **ENN**, the normalisation factor is: $16.84 \cdot 200 \cdot (42.64)^4 \cdot (175.9)^8 = 1.02E28$
So, the total sensitivity for station **ENN** is:

$$S = 570 \cdot 383 \cdot 1.4 \cdot 8 \cdot 204.8 \cdot 1.02E28 = \textbf{5.11E36} \text{ [Counts.s/m]}$$

No detailed sensitivity is known for stations **HEE** and **KRN**

Station ***VKB, RDC, SCHN, HGN***

All stations are using the same short period sensor, the Willmore Mk IIIa, which is characterized by a sensitivity of 520 Vs/m. The electronic amplification is equal to a factor 100. An additional external damping resistance is used (7 $k\Omega$), providing an attenuation

factor of 0.259 (7/(20+7)). Finally the same 16 bits A/D converter is used as in the borehole set-up with a gain setting of 3, meaning a factor 8, thus:

$$S = 520 \cdot 100 \cdot 0.259 \cdot 65536 \cdot 8/20 \cdot (175.9)^8 = 3.24E26 \text{ [Counts.s/m]}$$

Since the A/D card has 16 traces available, most stations record the same seismometer signal in 4 different gain settings. The first three with a factor 8, the next three with factor 4, the next three with a factor 2 and the last three traces with a factor 1.

4.5 Modification history and developments

The time of operation of the short period stations, their sampling rates and eigen periods are:

Station name	Operational since	Sampling rate	Z [s]	N [s]	E [s]
ENN (Mk II)	December 19, 1980 Closed end 1994?	120 Hz	1.0	-	-
KRN (Mk II)	March 18, 1985 Closed 1989?	120 Hz	1.0	-	-
HEE (MkIIIA)	December 19, 1980 Closed 31.12.1980	120 Hz	1.0	-	-
HEE (Mk II)	Open: 27-10-1972 Closed: 19.12.1980 Vm=12.000	120 Hz	1.5		
HGN (digital)	August 3 , 1995	120 Hz	0.96	1.92	1.56
VKB (MkIIIA)	May 22, 1985	120 Hz	1.0	-	-
VKB (digital)	September 10, 1996	120 Hz	1.0	1.25	1.25
RDC (digital)	December 13, 1996	120 Hz	0.9	1.44	1.35
SCHN (digital)	October 30, 2001	120 Hz	1.0	1.5	1.5

Since May 1, 2001 station **HGN** is equipped with a new set of electronics. One modification of the electronics was a change in value of the capacitor in the high pass filter (equation ***3.12***) from a value of 15 μF to a new value of 33 μF and thus changing the pole s_2 from a value of (0.666, 0.701) to a value of (0.303, 0.319). The value for ω_2 changes from a value of 0.967 (a cut-off frequency of 0.15 Hz) to a value of 0.440 (a cut-off frequency of 0.07 Hz). The same values are used for station **SCHN** from the start of its operation.

The Assen-array (stations **ZYN, WSB, RLD, LGV, BVS** and **MWD**) was operational from December 1988 until June 1994. Station **WIT** was equipped with a Willmore Mk II from June 29, 1978 until November 16, 1993. Station **WTS** was equipped with a Willmore Mk II from June 7, 1994 until late 2000.

4.6 Timing

At all stations a DCF-77 time receiver was deployed. Data from stations recording in a digital format at the station all have a separate time channel recorded. For the stations that did record in PCM form, time information is unreliable and should be compared to the data on paper.

4.7 Summary of response information

	Assen-array	WIT	WTS	ENN	HGN, VKB, RDC
S	9.28E32	1.95E33	5.84E33	5.11E36	3.24E26
np	16	15	15	16	12
s_1	(-4.21, 4.65)	(-3.52, 5.22)	(-3.52, 5.22)	(-5.22, 3.52)	(4.15, 4.71)
s_2	(-4.21, -4.65)	(-3.52, -5.22)	(-3.52, -5.22)	(-5.22,-3.52)	(4.15,-4.71)
s_3	(-31.45, 0.00)	(-16.84, 0.00)	(-13.78,0.00)	(-16.84,0.00)	(-0.666, 0.701)
s_4	(-0.67,0.00)	(-42.64,0.00)	(-42.64,0.00)	(-200., 0.00)	(-0.666, -0.701)
s_5	(-42.64,0.00)	(-42.64,0.00)	(-42.64,0.00)	(-42.64,0.00)	(-34.30, 172.52)
s_6	(-42.64,0.00)	(-42.64,0.00)	(-42.64,0.00)	(-42.64,0.00)	(-34.30, -172.52)
s_7	(-42.64,0.00)	(-42.64,0.00)	(-42.64,0.00)	(-42.64,0.00)	(-97.71, 146.26)
s_8	(-42.64,0.00)	(-34.30, 172.52)	(-34.30, 172.52)	(-42.64,0.00)	(-97.71, -146.26)
s_9	(-34.30, 172.50)	(-34.30, -172.52)	(-34.30, -172.52)	(-34.30, 172.52)	(-146.26, 97.72)
s_{10}	(-34.30, -172.52)	(-97.71, 146.26)	(-97.71, 146.26)	(-34.30, -172.52)	(-146.26, -97.72)
s_{11}	(-97.71, 146.26)	(-97.71, -146.26)	(-97.71, -146.26)	(-97.71, 146.26)	(-172.56, 34.13)
s_{12}	(-97.71, -146.26)	(-146.26, 97.72)	(-146.26, 97.72)	(-97.71, -146.26)	(-172.56, -34.13)
s_{13}	(-146.26, 97.72)	(-146.26, -97.72)	(-146.26, -97.72)	(-146.26, 97.72)	
s_{14}	(-146.26, -97.72)	(-172.56, 34.13)	(-172.56, 34.13)	(-146.26, -97.72)	
s_{15}	(-172.56, 34.13)	(-172.56, -34.13)	(-172.56, -34.13)	(-172.56, 34.13)	
s_{16}	(-172.56, -34.13)			(-172.56, -34.13)	
nz	4	4	4	4	5
z_1	(0.00, 0.00)	(0.00, 0.00)	(0.00, 0.00)	(0.00, 0.00)	(0.00, 0.00)
z_2	(0.00, 0.00)	(0.00, 0.00)	(0.00, 0.00)	(0.00, 0.00)	(0.00, 0.00)
z_3	(0.00, 0.00)	(0.00, 0.00)	(0.00, 0.00)	(0.00, 0.00)	(0.00, 0.00)
z_4	(0.00, 0.00)	(0.00, 0.00)	(0.00, 0.00)	(0.00, 0.00)	(0.00, 0.00)
z_5					(0.00, 0.00)

	HGN (2001/6/6), SCHN
S	6.71E25
np	12
s_1	(4.15, 4.71)
s_2	(4.15,-4.71)
s_3	(-0.303, 0.319)
s_4	(-0.303, -0.319)
s_5	(-34.30, 172.52)
s_6	(-34.30, -172.52)
s_7	(-97.71, 146.26)
s_8	(-97.71, -146.26)
s_9	(-146.26, 97.72)
s_{10}	(-146.26, -97.72)
s_{11}	(-172.56, 34.13)
s_{12}	(-172.56, -34.13)
nz	5
z_1	(0.00, 0.00)
z_2	(0.00, 0.00)
z_3	(0.00, 0.00)
z_4	(0.00, 0.00)
z_5	(0.00, 0.00)

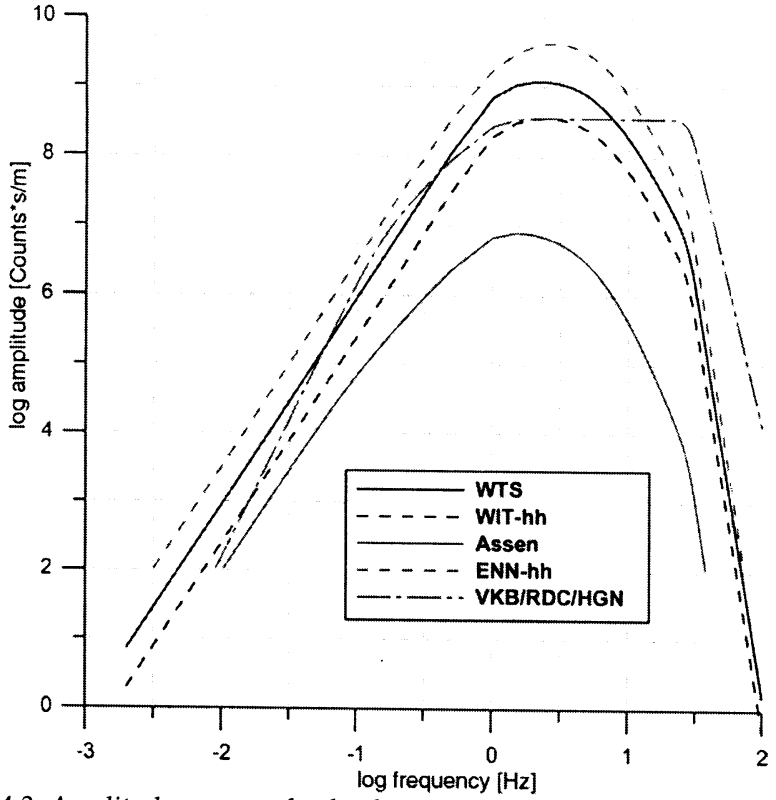

Figure 4.2. Amplitude response for the short period stations described in chapter 4.

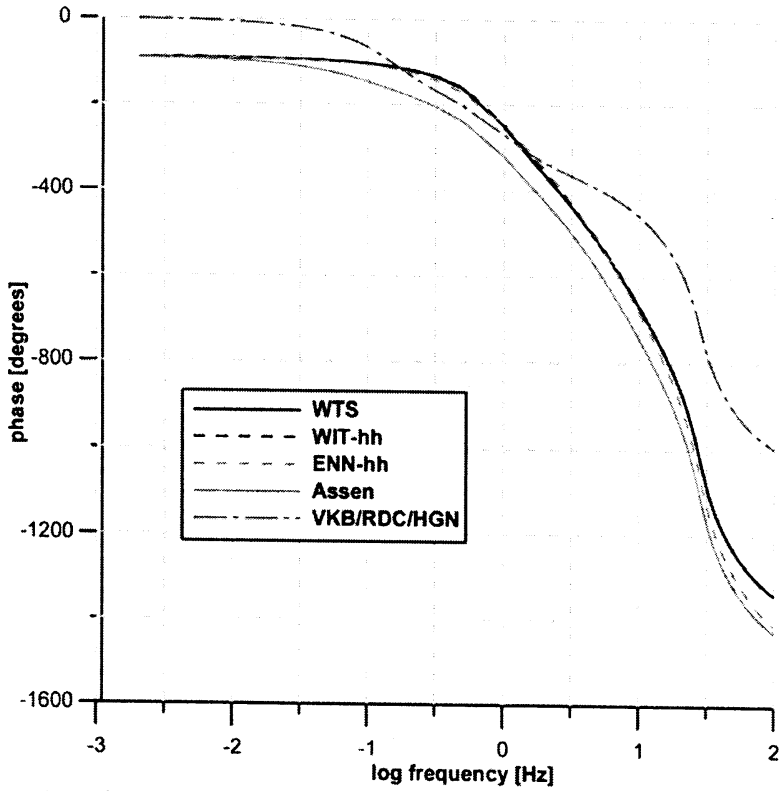

Figure 4.3. Phase response for the short period stations described in chapter 4

Figure 5.1. Overview of seismic stations in the Netherlands, installed and maintained by the KNMI (status: summer 2002). Long period surface station DBN is shown as a filled triangle.

5. Traditional analogue instrumentation at DBN

Several long period seismometers have been used in the history of the KNMI. Most requests for analogue data for historic events have been received for the Galitzin recordings. Two horizontal Galitzins were in operation since 1912, while one more vertical component was added in 1922. Recording was discontinued at December 16, 1994. In addition a Wiechert (NS and EW comp., 200 kg mass) and a Bosch (NS and EW component, 20kg mass) were in operation, both since 1908.

Recently an effort was made to scan and digitise Galitzin seismograms and therefore a description of the response is given in this chapter. In addition a digital system is described, which is still in operation at station DBN. Initially based on Press-Ewing sensors, but later replaced by a set of Teledyne-Geotech SL-210/220 sensors. This system can be used to simulate a Galitzin instrument and compare recent events to older ones.

5.1 Galitzin seismograph

The Galitzin system consists of an electro-magnetic seismograph combined with a galvanometer. The description of this system in terms of poles and zeroes (transfer function) is:

Seismograph response:

$$T_s(s) = \frac{s^3 S}{(s^2 + 2h_s\omega_s s + \omega_s{}^2)} \qquad 5.1$$

Galvanometer response:

$$T_g(s) = \frac{\gamma\omega_g{}^2}{(s^2 + 2h_g\omega_g s + \omega_g{}^2)} \qquad 5.2$$

Total response:

$$T_{tot}(s) = T_s(s) \cdot T_g(s) \qquad 5.3$$

In this formulation it is assumed that the coupling between seismometer and galvanometer is zero. Hagiwara (1958) showed that the coupling factor σ depends on the attenuation of the seismometer- galvanometer system. For a Galitzin configuration $\sigma \sim \mu$ and for the DBN system $\mu < 0.2$, which is sufficiently small to neglect coupling. Aki and Richards (1980) give a modern description of the seismometer-galvanometer system in chapter 10.3.3.

Galitzin (1914, pp 307-312) derived a formula for the gain V of a Galitzin seismograph:,

$$V = \frac{kA}{\pi l} \cdot \frac{T}{(1+u_1{}^2)(1+u^2)\sqrt{1-\mu^2 f(u)}} \qquad 5.4$$

where $f(u) = (\frac{2u}{1+u^2})^2$, $u = \frac{T}{T_s}$, $u_1 = \frac{T}{T_g}$, k denotes the transfer factor, A the distance between galvanometer mirror and the recording paper, l the reduced pendulum length, T the

period, T_s the eigenperiod of the seismometer and T_g the eigenperiod of the galvanometer. Since damping constant μ is close to zero and $T_s = T_g$, the expression can be rewritten as:

$$V = \frac{kA}{\pi l} \cdot \frac{T}{(1+u^2)^2} \qquad 5.5$$

and maximum gain ($T_m = \frac{1}{\sqrt{3}} T_s$):

$$V_m = \frac{kA}{\pi l} \cdot \frac{T_m}{(1+u^2)^2} = 0.56 \cdot \frac{kAT_m}{\pi l} \qquad 5.6$$

According to Kanamori (1988) peak magnification is equal to $V = \frac{0.32kAT_s}{\pi l}$, which is in agreement with equation **5.6**.

V is often defined as the maximum amplification, so one should select a normalisation constant at the period (T_m) where the response is a maximum. In the process of digitisation a conversion takes places from the recording on paper in cm to Digital Counts. This factor is indicated by S and given in Counts/m. For the 1932 Uden event the maximum amplitude on paper is 5.4 cm, which corresponds to a maximum of 29868.6 Counts.

The damping parameter h is measured through the parameter $\varepsilon^2 = 1 - h^2$. In the following table the parameters for the Galitzin recording are summarized for the Uden event (see Seismische Registr. In de Bilt, 1932):

Comp.	ε	k	A	$T_{s,g}$	l	V	S [Counts/m]	Norm. const.
Z	0.	175	1380	12.	405.9	727	5.53E6	1.614 (7s)
N	0.	11	1380	24.43	123.12	307	5.50E6	0.793 (14s)
E	0.	11	1380	24.96	122.58	315	5.70E6	0.793 (14s)

5.2 *Wiechert and Bosch seismographs*

Two horizontal Wiechert components and two horizontal Bosch components are recorded on smoked paper. The mass of the Wiechert seismograph is 200 kg and the Bosch 20 kg. Instrument parameters are published annually in the series Seismische Registr. In de Bilt. The transfer function for both seismographs is:

$$T_s(s) = \frac{s^2 V}{(s^2 + 2h_s\omega_s s + \omega_s^2)} \qquad 5.7$$

since the recording is a direct transfer of the mass movement to a drum. For the Wiechert instrument the parameter values for 1932 are:

component	T_0	V	ε	h
NS	5.0	162	4	0.404
EW	5.0	171	4	0.404

with $\omega_s = 2\pi / T_0$ and $\ln(\varepsilon) = \frac{\pi h}{\sqrt{1-h^2}}$ (see Kanamori, 1988 and Appendix A of this document).

For the Bosch the parameters are:

component	T_0	V	ε	h
NS	18.3	20.3	4	0.404
EW	18.5	20.3	4	0.404

The transfer functions for the Galitzin, Wiechert and Bosch instruments are shown in figure *5.1* and *5.2*.

	Galitzin-vert	**Galitzin-hor**	**Wiechert**	**Bosch**
S	727*1.614	311*0.793	165	20.3
np	4	4	2	2
s_1	(-0.524, 0.00)	(-0.257,0.00)	(-0.508,1.150)	(-0.139,0.314)
s_2	(-0524, 0.00)	(-0.257,0.00)	(-0.508,-1,150)	(-0.319,-0.314)
s_3	(-0524, 0.00)	(-0.257,0.00)		
s_4	(-0524, 0.00)	(-0.257,0.00)		
nz	3	3	2	2
z_1	(0.00, 0.00)	(0.00, 0.00)	(0.00, 0.00)	(0.00, 0.00)
z_2	(0.00, 0.00)	(0.00, 0.00)	(0.00, 0.00)	(0.00, 0.00)
z_3	(0.00, 0.00)	(0.00, 0.00)		

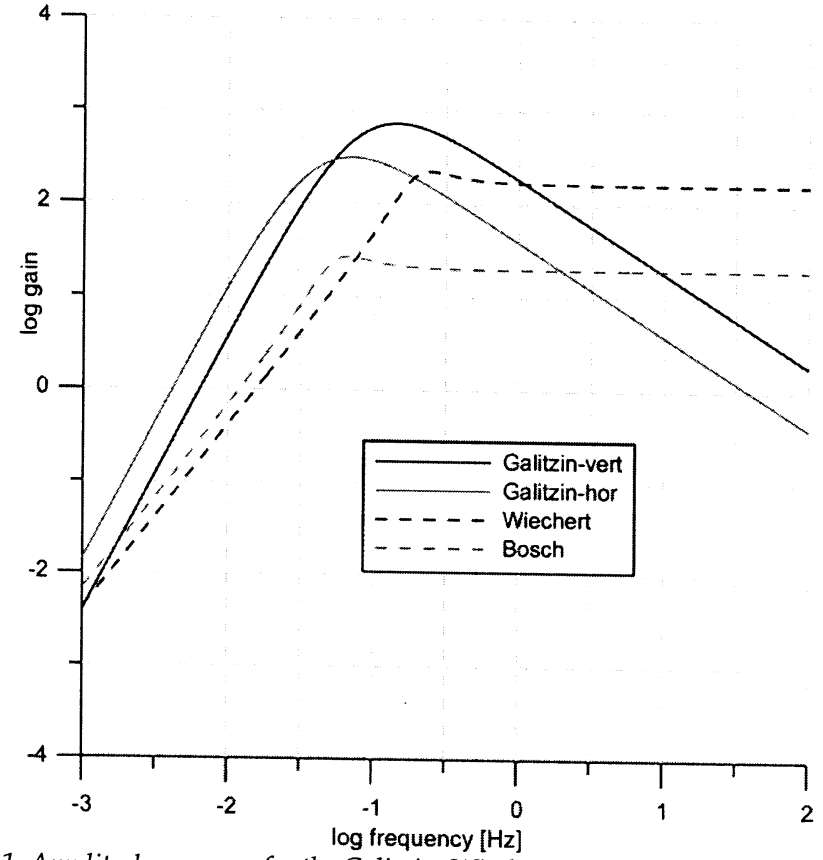

Figure 5.1. Amplitude response for the Galitzin, Wiechert and Bosch seismograph systems.

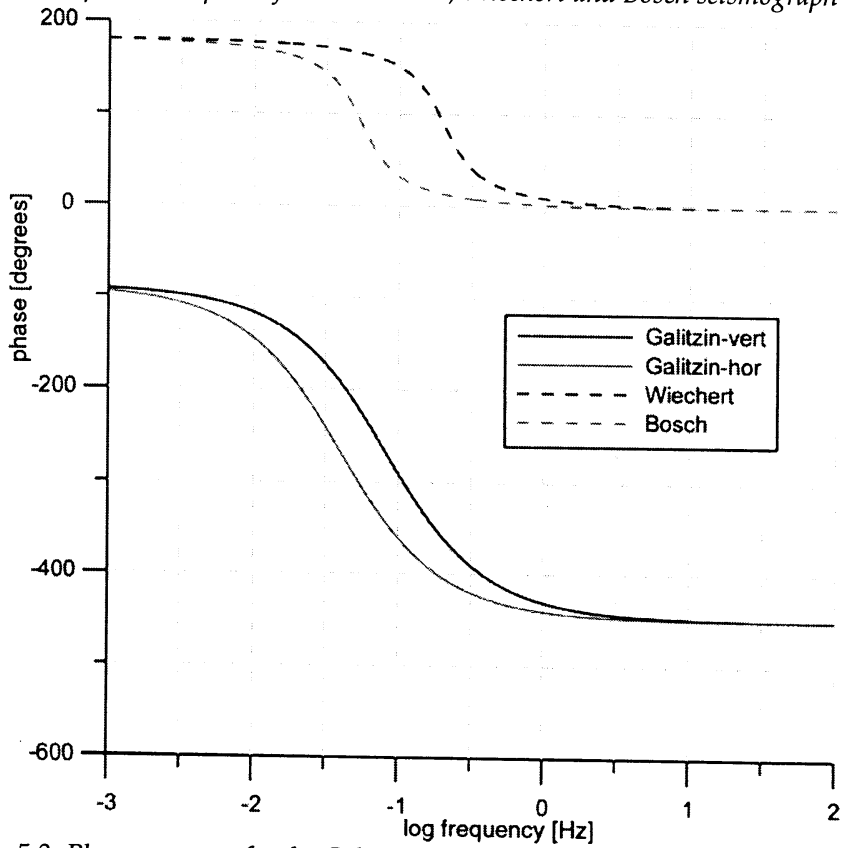

Figure 5.2. Phase response for the Galitzin, Wiechert and Bosch seismograph systems.

5.3 *Press-Ewing and Teledyne-Geotech seismographs*

In 1994 (November 22) a set of Press-Ewing seismographs, in operation at the KNMI, was adapted to digital recording. Unfortunately, the spring of the vertical sensor broke in 1995 (around October 15) and the vertical sensor was replaced (May 20, 1996) by a long period Teledyne-Geotech SL210 seismometer. The two horizontal component Press-Ewing sensors are replaced by two Teledyne-Geotech SL 220 horizontal sensors November 25, 1997.

5.3.1 *Sensor*

The transfer function of the sensor is given by:

$$T_s(s) = \frac{s^3 S_s}{s^2 + 2h_0\omega_0 s + \omega_0{}^2} \qquad 5.8$$

Following a discussion on the electromagnetic velocity sensor (Aki and Richards, 1980, pp 506-514; see also equation **4.3**), damping h_0 can be related to the generator constant (G), mass (M) and coil (R_0) and external resistor (R) by:

$$h_0 = \frac{\varepsilon}{\omega_0} = \frac{G^2}{2(R_0 + R)M\omega_0} \qquad 5.9$$

Press-Ewing:

The coil resistance is 520 Ω and the applied external damping resistor 1000 Ω. With a total mass of 7.5 kg, a generator constant of 96 Vs/m and an eigenperiod of 20 s, the value for ε = 0.404 and h_0 = 1.29. At critical damping (h_0=1) the Critical Damping Resistance (CDR) becomes 1956 Ω. The sensitivity is dependent on the CDR value used through the equation $G = \sqrt{4\pi f_0 M(CDR)}$ where f_0 is the eigenfrequency in Hz. Values for known eigenperiods are listed, assuming the same G for three components. All damping values are larger than 1.0.

Teledyne-Geotech:

External damping applied to this sensor is 6480 Ω (Z) and 6800 Ω (NS and EW), which is within the recommended CDR value (6440 Ω ± 10%; in general CDR in Ω should be 322* the natural period in seconds). Damping can be calculated using equation **5.9**, where R_0 = 1200 Ω and M= 2 kg.

Sensor/Component	Eigen period	Sensitivity (Vs/m)	h_0
Press-Ewing Z	18.5 sec	96	1.19
Press-Ewing N	21.7 sec	96	1.40
Press-Ewing E	26.7 sec	96	1.72
Teledyne-Geotech SL-210 (Z)	20.5	90	0.86
Teledyne-Geotech SL-220 (N)	20.	94	0.88
Teledyne-Geotech SL-220 (E)	20.	94	0.88

5.3.2 *Anti-aliasing filters*

Similar to the borehole electronics, an 8th order Butterworth filter (equation *3.13*) is applied at a corner frequency of 5 Hz. The only other component of interest is a gain factor of 219 that is applied in the total electronics scheme.

5.3.3 *Total transfer function*

$$T_{tot}(s) = T_s(s) \cdot T_{al}(s)$$

$$T_{tot}(s) = \frac{Ss^3}{(s^2 + 2h_0\omega_0 s + \omega_0{}^2)} \cdot \prod_{k=1}^{4} \frac{\omega_1{}^2}{s^2 + 2h_k\omega_1 s + \omega_1{}^2}$$

$$T_{tot}(s) = \frac{Ss^3}{(s - s_1)(s - s_1{}^*)} \cdot \prod_{k=1}^{4} \frac{\omega_1{}^2}{(s - s_{k+1})(s - s_{k+1}{}^*)}$$

with

s_2= (- 6.13, 30.81)
s_3= (-17.45, 26.12)
s_4= (-26.12, 17.45)
s_5= (-30.82, 6.09)

Since damping values for the Press-Ewing are larger than one, the seismometer poles are real valued. An overview of values for s_1 is given in the response overview, following the Sensitivity discussion.

5.3.4 *Sensitivity*

The total sensitivity is: $S = S_S \cdot 219 \cdot 32768/20 = S_S \cdot 3.59E05\ [Counts \cdot s/m]$. Normalisation constant is $(31.42)^8$ = 9.50E11. The sampling rate used is 20 Hz

	Press-Ewing	**Press-Ewing**	**Press-Ewing**	**Teledyne-Geotech**	**Teledyne-Geotech**	**Teledyne-Geotech**
	Z	**NS**	**EW**	**Z**	**NS**	**Z**
S	3.27E19	3.27E19	3.27E19	3.07E19	3.21E19	3.21E19
np	10	10	10	10	10	10
s_1	(-0.624, 0.00)	(-0.690, 0.00)	(-0.733, 0.00)	(-0.263, 0.156)	(-0.276, 0.149)	(-0.276, 0.149)
s_2	(-0.186, 0.00)	(-0.122, 0.00)	(-0.075, 0.00)	(-0.263, -0.156)	(-0.276, -0.149)	(-0.276, -0.149)
s_3	(-6.13, 30.81)	(-6.13, 30.81)	(-6.13, 30.81)	(-6.13, 30.81)	(-6.13, 30.81)	(-6.13, 30.81)
s_4	(-6.13, -30.81)	(-6.13, -30.81)	(-6.13, -30.81)	(-6.13, -30.81)	(-6.13, -30.81)	(-6.13, -30.81)
s_5	(-17.45, 26.12)	(-17.45, 26.12)	(-17.45,26.12)	(-17.45, 26.12)	(-17.45, 26.12)	(-17.45, 26.12)
s_6	(-17.45,-26.12)	(-17.45, -26.12)	(-17.45, -26.12)	(-17.45, -26.12)	(-17.45, -26.12)	(-17.45, -26.12)
s_7	(-26.12, 17.45)	(-26.12, 17.45)	(-26.12, 17.45)	(-26.12, 17.45)	(-26.12, 17.45)	(-26.12, 17.45)
s_8	(-26.12, -17.45)	(-26.12, -17.45)	(-26.12,-17.45)	(-26.12, -17.45)	(-26.12, -17.45)	(-26.12, -17.45)
s_9	(-30.82, 6.09)	(-30.82, 6.09)	(-30.82, 6.09)	(-30.82, 6.09)	(-30.82, 6.09)	(-30.82, 6.09)
s_{10}	(-30.82, -6.09)	(-30.82,-6.09)	(-30.82,-6.09)	(-30.82, -6.09)	(-30.82, -6.09)	(-30.82, -6.09)
nz	3	3	3	3	3	3
z_1	(0.00, 0.00)	(0.00, 0.00)	(0.00, 0.00)	(0.00, 0.00)	(0.00, 0.00)	(0.00, 0.00)
z_2	(0.00, 0.00)	(0.00, 0.00)	(0.00, 0.00)	(0.00, 0.00)	(0.00, 0.00)	(0.00, 0.00)
z_3	(0.00, 0.00)	(0.00, 0.00)	(0.00, 0.00)	(0.00, 0.00)	(0.00, 0.00)	(0.00, 0.00)

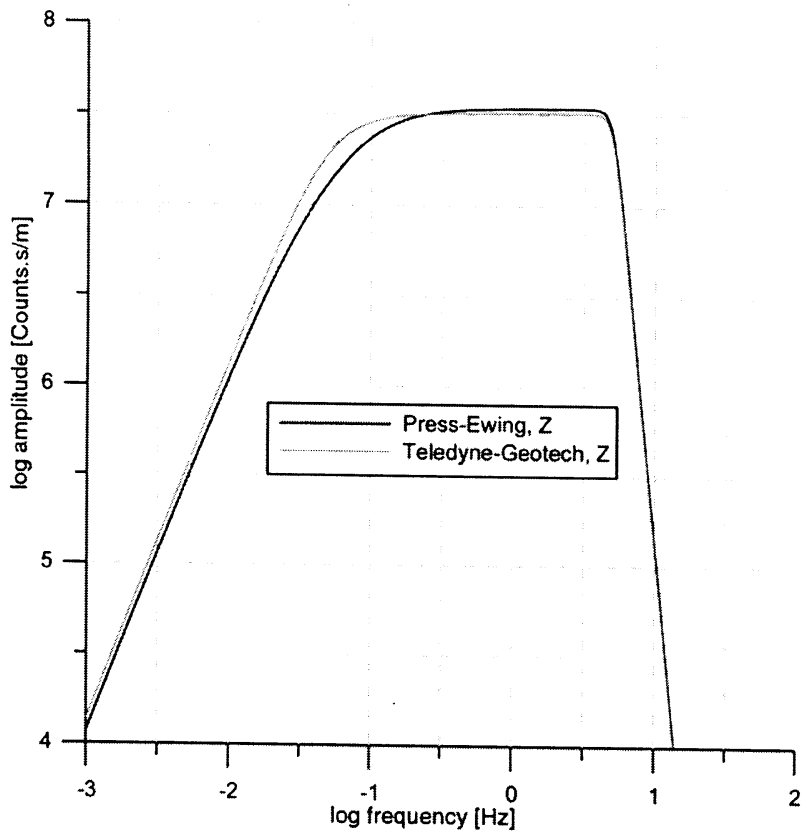

Figure 5.3 Amplitude response for the Teledyne-Geotech and Press-Ewing seismographs

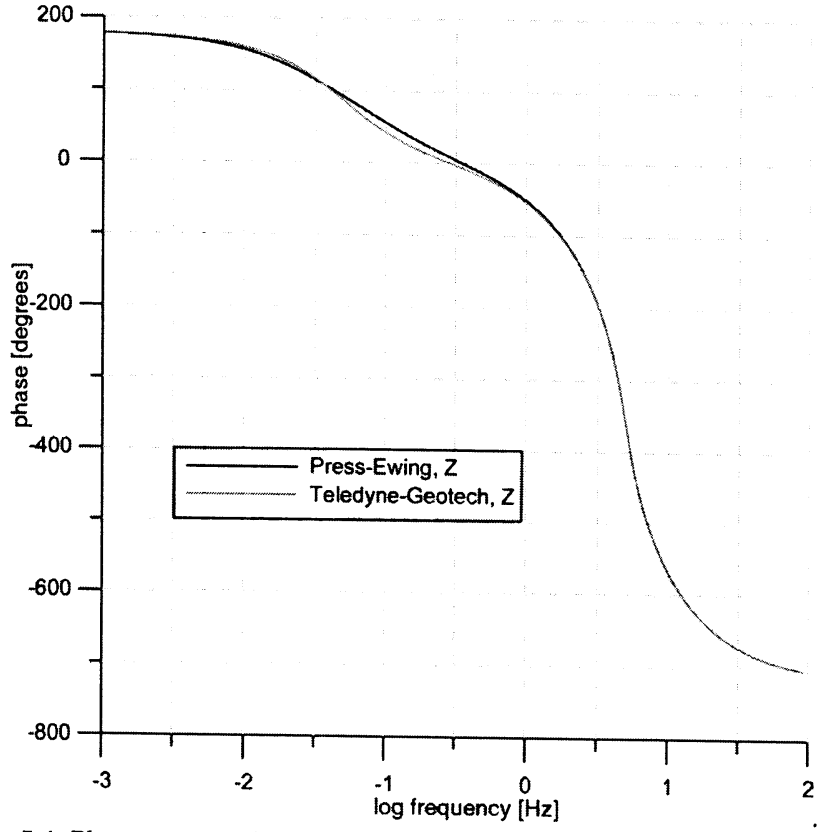

Figure 5.4. Phase response for the Teledyne-Geotech and Press-Ewing seismographs

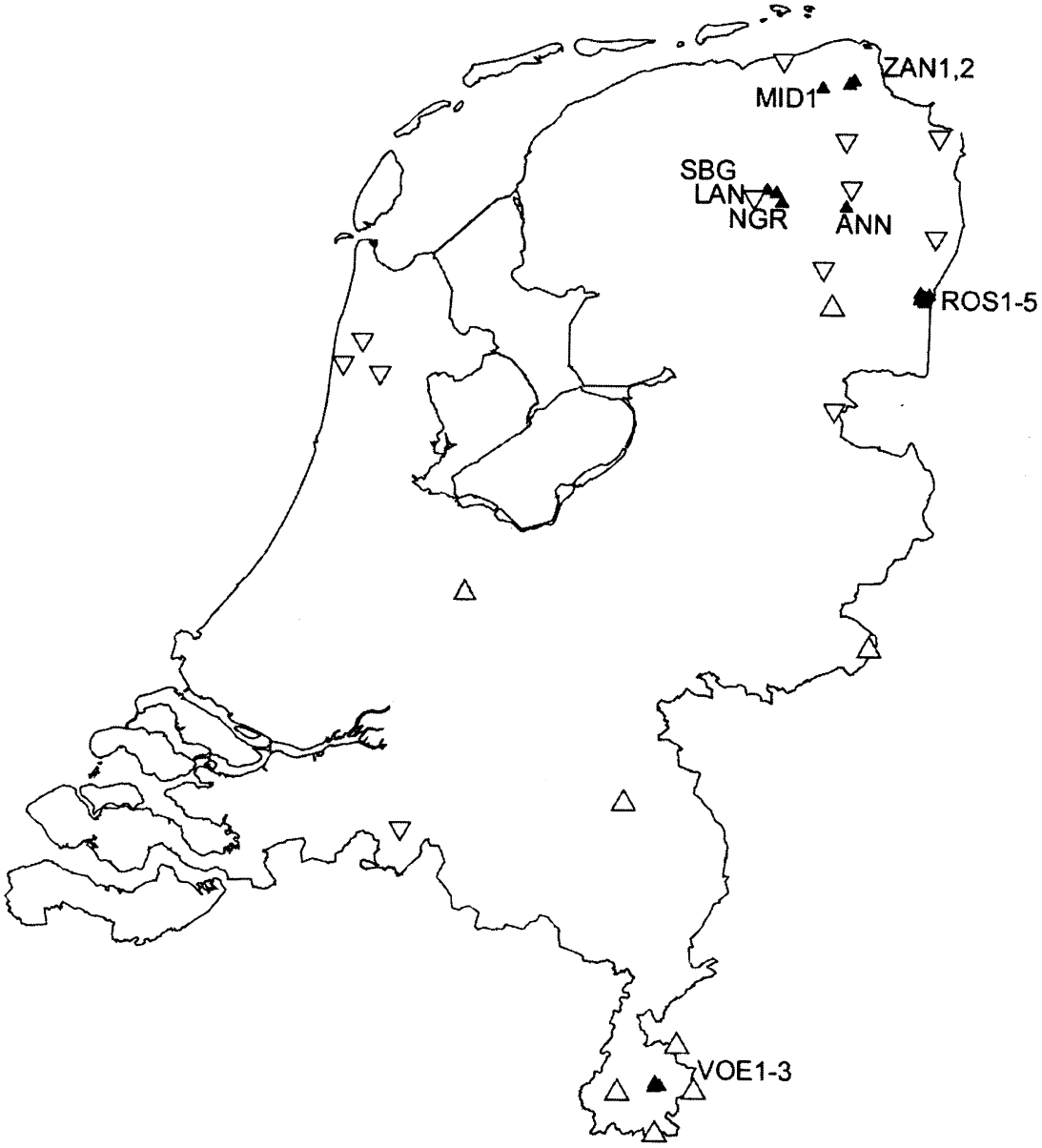

Figure 6.1. Overview of seismic stations in the Netherlands, installed and maintained by the KNMI (status: summer 2002). Accelerometer stations are shown as filled triangles.

6. Accelerometers

The accelerometers used by the KNMI are SIG AC-23 sensors in combination with a SMACH2 datalogger. The sensor itself is characterized by a one pole high-pass filter at a corner frequency of 0.2 Hz and a 2 pole Bessel low-pass filter at 50 Hz. The data logger samples at 200 Hz through a digital Hogenauer (FIR) filter. This filter has a 3 dB point at 0.262*sampling rate (= 52.4 Hz) and thus reinforces the low-pass Bessel filter function.

6.1 Sensor

The transfer function for the SC-23 (for displacement) is:

$$T_{acc}(s) = \frac{s^3 S}{s+\omega_0} \cdot \frac{\omega_1^{\,2}}{s^2 + 2.208\omega_1 s + 1.624\omega_1^{\,2}} = \frac{s^3 S}{(s-s_1)} \cdot \frac{\omega_1^{\,2}}{(s-s_2)(s-s_2^{\,*})} \qquad 6.1$$

where ω_0 = 1.26 rad/s, ω_1 = 314.16 rad/s, S varies depending on the setting at the station. The setting can be read from the header to the data. Data on disk are in [mg].

s_1 = (-1.257, 0.00)
s_2 = (-346.83, 200.12)

6.2 Data logger

The data logger is a 16-bit A/D board (based on delta-sigma conversion) and only adds a digital filter from the decimation process (64kHz down to 200 Hz sampling). The filter is an Hogenauer filter or CIC filter (Garcia et al, 1998) and its frequency characteristic is given by:

$$T(z) = \left(\frac{1-z^{-RD}}{1-z^{-1}}\right)^T \qquad 6.2$$

with R= sampling rate reduction, D=differential delay (design parameter) and T= number of cascaded comb stages. In our case there are three stages (T = 3) with a total sampling rate reduction of 320 (R = 8,8 and 5) and D is taken to be 1. Equation 6.2 is evaluated for $z = e^{s/R}$ and then shows a frequency response relative to the low sampling rate.

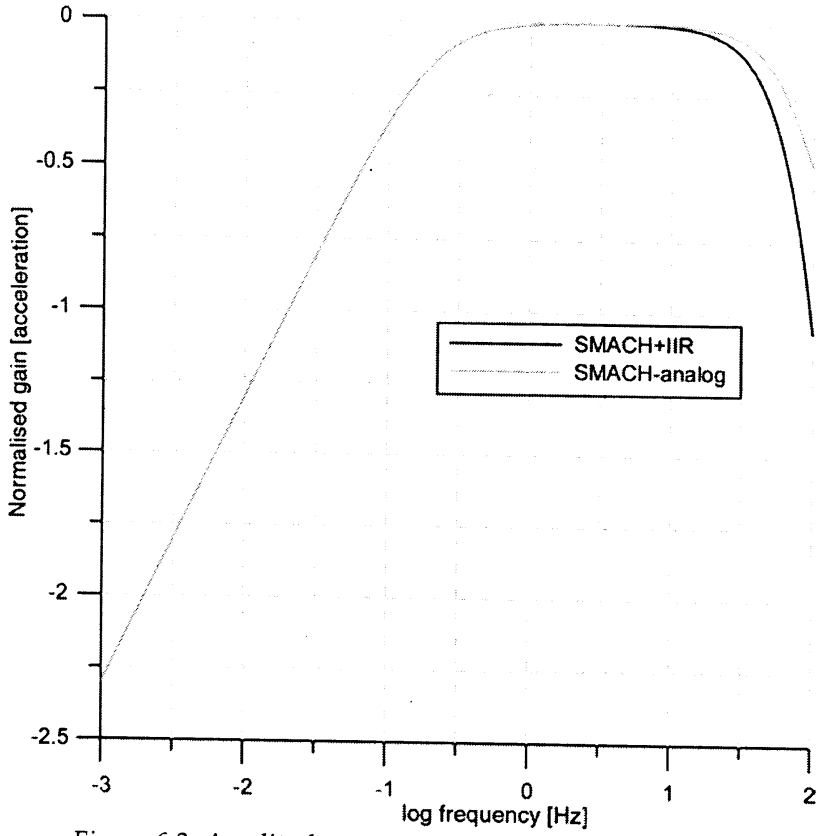

Figure 6.2. Amplitude response of the accelerometer system

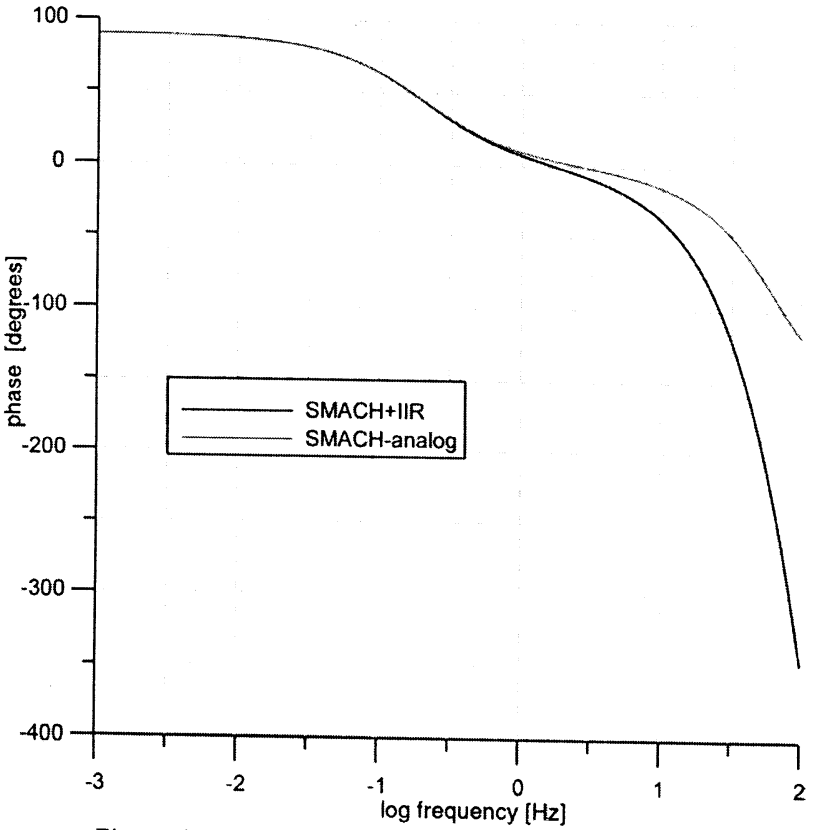

Figure 6.3. Phase response of the accelerometer system

7. References

Aki, K. and P. Richards, 1980, Quantitative Seismology; Theory and Methods, vol 1, Freeman and Company, San Francisco, 557 pp.

Dost, B., A. van Wettum and G. Nolet, 1984, The NARS array, Geol. Mijnbouw, 63, pp 381-386

Garcia, A., U. Meyer-Baese and F. Taylor, 1998,
Pipelined Hogenauer CIC Filters using Field-Programmable Logic and Residue Number System. International Conference on Acoustics, Speech, and Signal Processing, May, 1998, Seattle, Vol. 5, pp. 3085-3088

Hutt, C.R., 1993, Specifying and using channel response information, Appendix C in: Standards for the Exchange of Earthquake Data (SEED) reference manual, pp 203.

Kanamori, H., 1988, Importance of Historical Seismograms for Geophysical Research in: Historical seismograms and earthquakes of the world, ed. Lee, W.H.K., H. Meijers and K. Shimazaki, Academic Press, pp 16-36

Seidl, 1980, The Simulation Problem for Broad-Band Seismograms, J. Geophys., **48**, pp 84-93.

Seidl, D. and W. Stammler, 1984,Restoration of broad-band seismograms (Part I), J. Geophys., **54**, pp 114-122.

Seismische Registrierungen. In de Bilt, 1934, vol 20, KNMI series nr 108, Rijksuitgeverij 'sGravenhage 52 pp.

Wielandt, E., 2001, Seismic Sensors and their Calibration, In: Manual of Observatory Practice, Edited by Peter Bormann and Erik Bergmann. (http://www.geophys.uni-stuttgart.de/skripten/index.html)

Wielandt, E. and J.M. Steim, 1985, A digital very-broad-band seismograph, Annales Geophysicae, 4, B, 3, 227-232

Wielandt, E. and G. Streckeisen, 1982, The leaf-spring seismometer: design and performance, Bull. of the Seismological Soc. of Am., **72**, pp 2349-2367

Appendix A: DBN Galitzin calibration values

This document describes the calibration of the Galitzin seismograph operated at station DBN by the KNMI in de Bilt. Calibration of the instrument was focused on the determination of the gain of the instrument as a function of frequency and especially the peak magnification, which is an essential parameter in a description of the instrument in terms of poles and zeroes.

Galitzin (1914, pp 307-312) derived a formula for the gain V of a Galitzin seismograph:

$$V = \frac{kA}{\pi l} \cdot \frac{T}{(1+u_1^{\,2})(1+u^2)\sqrt{1-\mu^2 f(u)}} \qquad \textit{A.1.1}$$

where $f(u) = (\frac{2u}{1+u^2})^2$, $u = \frac{T}{T_s}$, $u_1 = \frac{T}{T_g}$,

k denotes the transfer factor, A the distance between galvanometer mirror and the recording paper, l the reduced pendulum length, T the period, T_s the eigen period of the seismometer and T_g the eigen period of the galvanometer. Since damping constant μ is close to zero and $T_s = T_g$, the expression can be rewritten as:

$V = \frac{kA}{\pi l} \cdot \frac{T}{(1+u^2)^2}$ and maximum gain ($T_m = \frac{1}{\sqrt{3}} T_s$):

$$V_m = \frac{kA}{\pi l} \cdot \frac{T_m}{(1+u^2)^2} = 0.56 \cdot \frac{kAT_m}{\pi l} \qquad \textit{A.1.2}$$

According to Kanamori (1988) seismograph gain is equal to $V = \frac{0.32kAT_s}{\pi l}$, which is in agreement with equation ***A.1.2.***

The parameters for the reduced pendulum length are constant (NS: l= 123.13 mm, EW: l= 122.58 mm and Z: l= 405.9 mm), together with the galvanometer eigenperiod (NS: T_g= 24.43 s, EW: T_g= 24.43 s and Z: T_g= 12.0 s). The other parameters (T_s, μ , k and A) are measured on a regular basis for the horizontal components, while only k is measured for the vertical component. An overview of these measurements is given in table 1 and 2. Table 1 gives the variations in annual values, while table 2 gives detailed information for the period 1914-1930. After 1945 only general values are specified.

Please note that major changes in the parameters did occur on September 19, 1917, when the factor k was modified from a value of 17 to 11. Another change was made July 31, 1918 when the factor A was modified from 1350 mm to 1380 mm.

References

Galitzin, Fuerst B., 1914, Vorlesungen ueber Seismometrie, Ed. O. Hecker, Teubner, Leipzig und Berlin, pp 538.

Kanamori, H., 1988, Historical seismograms and Earthquakes of the World, Ed. Lee, W.H.K, H. Meyers and K. Shimazaki, Academic Press, pp 513.

Table 1. Summary of calibration values per year

	Seismometer 32 (NS)				Seismometer 31 (EW)				Seismometer (Z)			
Date	T [s]	μ^2	k	A [mm]	T [s]	μ^2	k	A [mm]	T [s]	μ^2	k	A [mm]
1914	24.16	0.02	15.80	1351	24.49	0.03	14.70	1360				
	24.45	0.03	16.90		25.36	0.10	17.30					
1915	23.85	-0.19	13.42	1353	24.40	-0.04	12.85	1359				
	26.07	0.13	17.43		25.24	0.13	17.35					
1916	23.81	-0.06	16.12	1348	24.81	-0.07	16.41	1361				
	24.87	0.09	17.25		25.65	0.07	17.45					
1917-19/09	23.80	-0.06	16.12	1351	24.72	-0.05	15.95	1359				
	24.78	0.06	17.27		25.24	0.05	17.33					
1917 19/09-	23.80	-0.04	10.51		24.65	-0.03	11.09					
	24.72	0.03	11.02		24.96	0.02	11.14					
1918	23.93	-0.07	10.64	1350	24.74	-0.04	10.54	1359				
	25.01	0.07	11.13		25.32	0.08	11.22					
1918 31/07-				1378				1380				
1919	23.77	-0.07	10.37		24.72	-0.06	10.60					
	24.89	0.08	11.03		25.43	0.03	11.14					
1920	23.92	-0.06	10.67	1379	25.07	-0.07	10.77	1381				
	24.84	0.04	11.02		25.43	0.04	11.21					
1921	23.94	-0.04	10.60	1378	24.83	0.00	10.77	1379				
	24.36	0.06	10.97		25.23	0.08	11.17					
1922	23.82	-0.05	10.58	1376	24.38	-0.06	10.63	1380	12.0	0.0	*	1377
	24.36	0.07	10.92		25.32	0.06	11.19					
1923	23.43	-0.09	10.86	1376	24.48	-0.08	10.78	1379	12.0	0.0	170.1**	1377
	24.65	0.16	11.21		25.30	0.07	11.26				178.0	

*) For Oct 12-13, 1922 k=225; Oct 13-14 k= 199; Oct 14-2Feb 1923: k=225

**) For Jan 1-Feb 2, 1923 k=225; Feb 2-Feb 7 k=173; Feb 7-March 9 k=137. After March 9: 175

	Seismometer 32 (NS)				Seismometer 31 (EW)				Seismometer (Z)			
Date	T [s]	μ^2	k	A [mm]	T [s]	μ^2	k	A [mm]	T [s]	μ^2	k	A [mm]
1924	23.77	-0.05	10.91	1376	24.79	-0.04	10.90	1378	12.0	0.0	171.7	1376
	24.74	0.03	11.09		25.21	0.04	11.25				178.7	
average											175	
1925	22.67	-0.09	10.59	1380	24.68	-0.07	10.64		12.0	0.0	171.8	1376
	25.14	0.03	11.14		25.43	0.06	11.25				178.7	1380
average											175	
1926	22.74	-0.03	10.58	1380	23.71	-0.15	10.79	1380	12.0	0.0	169.6	1380
	24.92	0.21	11.13		26.36	0.16	11.20				178.5	
average											175	
1927	23.92	-0.01	10.44	1380	24.83	-0.05	10.72	1380	12.0	0.0	175.3	1380
	24.80	0.13	11.11		25.26	0.08	11.24				178.5	
average											177	
1928	24.18	-0.04	11.04	1380	24.43	-0.04	10.83	1380	12.0	0.0	173.5	1380
	24.63	0.10	11.13		25.33	0.09	11.20				179.5	
average											177	
1929	24.04	-0.02	10.47	1380	25.16	-0.04	10.19	1380	12.0	0.0	172.7	1380
	24.89	0.12	11.08		25.60	0.10	11.22				179.5	
average											177	
1930	24.14	-0.04	10.89	1380	24.26	-0.01	10.74	1380	12.0	0.0	169.6	1380
	25.09	0.05	11.12		25.56	0.19	11.28				178.5	
average											176	
1931	24.23	-0.04	10.93	1380	25.08	-0.04	10.89	1380	12.0	0.0	174.9	1380
	25.03	0.06	11.04		25.70	0.05	11.13				177.7	
average											176	
1932	23.94	-0.04	10.79	1380	24.56	-0.08	10.73	1380	12.0	0.0	170.9	1380
	24.72	0.07	11.04		25.58	0.13	11.18				178.5	
average											175	
1933	23.82	-0.09	10.79	1380	24.78	-0.05	10.36	1380	12.0	0.0	168.0	1380
	24.89	0.06	11.01		25.48	0.10	11.12				178.5	
average											173	
1934	23.92	-0.05	10.74	1380	24.61	-0.03	10.48	1380	12.0	0.0	168.0	1380
	24.81	0.05	11.02		25.60	0.08	11.11				177.1	
average											174	

	Seismometer 32 (NS)				Seismometer 31 (EW)				Seismometer (Z)			
Date	T [s]	μ^2	k	A [mm]	T [s]	μ^2	k	A [mm]	T [s]	μ^2	k	A [mm]
1935	24.06	-0.10	10.42	1380	24.38	-0.10	10.51	1380	12.0	0.0	173.7	1380
	25.21	0.09	10.98		26.03	0.15	11.07				177.8	
average											177	
1936	23.01	-0.07	10.71	1380	24.71	-0.05	10.65	1380	12.0	0.0	172.4	1380
	25.36	0.12	10.98		25.56	0.16	11.10				178.3	
average											177	
1937	23.89	-0.03	10.30	1380	24.53	-0.04	10.50	1380	12.0	0.0	171.4	1380
	25.39	0.10	11.01		26.16	0.17	11.14				178.3	
average											177	
1938	23.50	-0.12	10.61	1380	24.79	-0.08	10.15	1380			171.4	
	25.33	0.05	10.95		25.28	0.05	11.07				178.1	
average											175	
1939	23.62	-0.14	10.45	1380	24.53	-0.04	10.26	1380	12.0	0.0	174	1380
	24.99	0.14	10.98		25.28	0.07	11.08					
1940	24.28	-0.04	10.36	1380	24.33	-0.08	10.48	1380	12.0	0.0	175	1380
	24.77	0.09	10.98		24.93	0.06	11.05					
1941	23.80	-0.08	09.69	1380	24.56	0.00	10.36	1380	12.0	0.0	178	1380
	26.82	0.17	11.24		27.10	0.23	10.90					
1942	21.00	-0.13	10.52	1380	23.20	-0.01	10.03	1380	12.0	0.0	178	1380
	22.73	0.14	10.84		25.45	0.15	11.12					
1943	21.45	-0.08	10.62	1380	22.20	0.04	10.76	1380	12.0	0.0	178	1380
	23.25	0.05	11.18		23.95	0.14	11.21					
1944	23.20	-0.06	10.76	1380	23.25	-0.10	10.35	1380	12.0	0.0	178	1380
	25.40	0.14	11.30		26.18	-0.02	11.18					
1945	25	0.0	11.0	1380	25	0.0	11	1380	12.0	0.0	178	1380

Table 2. Detailed calibration measurements

Seism 32 (NS)					Seism. 31 (EW)				
Date	T [s]	μ^2	k	A [mm]	Date	T [s]	μ^2	k	A [mm]
03-04-1914	24.16	0.03	16.78		01-04-1914	24.49	0.03	17.30	
14-05-1914				1351					1360
30-07-1914	24.41	0.02	15.80		29-07-1914	25.36	0.10	14.70	
30-07-1914	24.45	0.03	16.90		29-07-1914	24.49	0.06	17.22	
20-01-1915	26.07	-0.19	13.42		19-01-1915	25.08	-0.04	12.85	
20-01-1915	24.38	-0.01	17.43		20-01-1915	25.21	0.09	17.33	
27-01-1915				1353					1359
24-03-1915	23.99	0.02	16.92		23-03-1915	24.83	0.01	17.31	
24-03-1915	23.99	0.02	16.92		23-03-1915	24.83	0.01	17.31	
11-05-1915	23.86	0.13	16.89		10-05-1915	24.93	0.13	16.43	
11-05-1915	23.98	-0.06	17.29		10-05-1915	24.53	0.00	17.33	
23-06-1915	23.88	-0.01	16.64		22-06-1915	24.40	0.05	16.70	
23-06-1915	23.85	0.03	16.58		22-06-1915	24.67	-0.03	17.35	
30-09-1915	23.91	0.01	16.97		29-09-1915	24.86	0.00	17.30	
30-09-1915	23.86	0.01	16.82		29-09-1915	24.99	-0.01	17.32	
25-10-1915	24.13	-0.03	16.69		25-10-1915	24.69	-0.05	17.29	
25-10-1915	24.12	0.09	17.01		25-10-1915	24.92	0.03	17.30	
22-11-1915	24.01	0.04	16.55		22-11-1915	24.82	0.04	16.41	
22-11-1915	23.96	0.04	16.96		22-11-1915	25.24	0.01	17.20	
22-02-1916	23.82	0.02	17.17		22-02-1916	25.31	-0.02	17.34	
22-02-1916	23.88	0.05	17.04		22-02-1916	25.28	-0.00	17.31	
30-03-1916	24.01	0.05	17.04		30-03-1916	25.39	-0.02	17.36	
30-03-1916	23.89	0.02	16.87		30-03-1916	25.31	-0.03	17.33	
02-05-1916	23.97	0.09	16.81		02-05-1916	25.65	0.07	16.41	
03-05-1916	24.33	-0.05	16.77		02-05-1916	25.41	-0.07	17.02	
03-05-1916				1348					1361
30-05-1916	23.99	-0.02	17.09		30-05-1916	25.38	-0.03	17.27	
30-05-1916	23.81	-0.04	17.25		30-05-1916	25.29	-0.04	17.40	
03-08-1916	24.09	0.03	16.68		03-08-1916	25.37	0.01	16.88	
03-08-1916	24.18	-0.03	17.10		03-08-1916	25.34	-0.00	17.41	
27-09-1916	24.76	-0.06	16.89		27-09-1916	25.29	-0.03	17.45	
27-09-1916	24.81	0.04	16.95		27-09-1916	25.42	0.04	17.23	
16-11-1916	24.61	-0.00	16.56		15-11-1916	25.12	0.05	17.23	
16-11-1916	24.25	0.01	16.96		15-11-1916	25.22	0.05	17.12	
21-11-1916				1350					1359
06-12-1916	24.61	-0.01	16.20		06-12-1916	24.86	0.03	16.78	
07-12-1916	24.87	0.05	16.70		06-12-1916	25.12	-0.01	17.21	
09-02-1917	24.77	-0.06	16.12		08-02-1917	24.81	-0.03	16.99	

Seism 32 (NS)					Seism. 31 (EW)				
Date	T [s]	μ^2	k	A [mm]	Date	T [s]	μ^2	k	A [mm]
09-02-1917	24.50	-0.06	16.82		09-02-1917	25.06	-0.03	17.09	
04-04-1917	24.18	0.02	17.13		04-04-1917	25.22	0.02	16.88	
05-04-1917	23.92	-0.03	17.27		04-04-1917	25.24	-0.05	17.33	
16-05-1917	23.94	0.05	16.82		15-05-1917	25.16	0.04	16.07	
16-05-1917	24.04	-0.04	17.13		15-05-1917	24.72	-0.03	17.29	
15-06-1917	23.95	0.06	16.03		14-06-1917	25.13	0.05	15.95	
15-06-1917	24.09	-0.02	16.69		14-06-1917	25.15	0.00	17.22	
19-09-1917	24.50	-0.03	16.44		17-09-1917	24.86	0.00	17.19	
19-09-1917	24.27	0.03	10.65		17-09-1917	24.86	0.02	11.14	
01-11-1917	23.80	-0.04	10.51		31-10-1917	24.65	-0.03	11.14	
01-11-1917	24.72	0.01	11.02		31-10-1917	24.96	0.02	11.09	
28-11-1917				1351					1359
04-01-1918	24.06	-0.04	10.64		03-01-1918	24.53	0.01	10.63	
05-01-1918	24.31	0.01	11.05		04-01-1918	24.79	-0.01	11.12	
19-03-1918	25.01	0.03	11.05		18-03-1918	24.74	0.02	10.94	
19-03-1918	24.80	-0.03	11.04		18-03-1918	24.89	-0.04	11.21	
14-05-1918	24.25	0.02	11.12		13-05-1918	24.83	0.02	10.95	
14-05-1918	24.35	-0.01	11.10		13-05-1918	25.19	-0.04	11.22	
29-07-1918	24.08	0.07	11.02		29-07-1918	25.32	0.07	10.54	
30-07-1918				1350					1359
31-07-1918				1378					1380
31-07-1918	24.10	0.01	11.00		31-07-1918	25.16	0.00	11.15	
06-09-1918	24.33	-0.04	11.08		05-09-1918	24.89	-0.03	11.21	
06-09-1918	24.32	0.02	11.02		05-09-1918	25.16	0.01	11.16	
06-09-1918				1377					1379
25-10-1918	24.65	0.00	10.81		24-10-1918	24.53	0.02	11.20	
25-10-1918	24.40	0.03	11.13		24-10-1918	24.81	0.02	11.16	
13-12-1918	24.00	0.02	10.96		12-12-1918	24.79	0.08	10.78	
13-12-1918	23.93	0.01	11.08		13-12-1918	25.12	0.04	11.12	
13-02-1919	24.05	-0.07	10.37		12-02-1919	24.72	-0.02	10.82	
13-02-1919	23.81	-0.04	10.97		12-02-1919	24.92	-0.02	10.91	
01-04-1919	23.91	0.04	11.02		26-03-1919	25.04	0.01	10.66	
01-04-1919	23.99	-0.02	11.03		26-03-1919	25.09	-0.06	11.14	
16-05-1919	23.77	0.08	10.88		15-05-1919	24.81	0.03	10.60	
16-05-1919	23.92	-0.02	10.80		15-05-1919	24.84	-0.06	10.97	
11-07-1919	23.92	0.04	10.74		10-07-1919	25.21	0.01	10.63	
11-07-1919	24.01	0.00	10.75		10-07-1919	25.19	-0.02	10.84	
04-09-1919	23.99	0.07	10.67		03-09-1919	25.16	0.00	10.78	
04-09-1919	23.98	0.08	10.78		03-09-1919	24.97	0.00	11.07	
22-10-1919	24.14	0.02	10.45		24-10-1919	24.91	-0.03	10.77	

Seism 32 (NS)					Seism. 31 (EW)				
Date	T [s]	μ^2	k	A [mm]	Date	T [s]	μ^2	k	A [mm]
22-10-1919	24.30	0.00	10.77		24-10-1919	25.43	0.00	10.67	
28-11-1919	24.65	-0.06	10.73		27-11-1919	25.18	-0.02	10.76	
28-11-1919	24.89	0.01	10.80		27-11-1919	25.23	0.00	10.73	
23-03-1920	24.02	0.02	10.86		22-03-1920	25.07	-0.01	10.77	
23-03-1920	24.11	-0.02	10.76		22-03-1920	25.16	-0.03	10.80	
03-05-1920				1378	03-05-1920				1380
25-05-1920	23.92	0.03	11.02		21-05-1920	25.42	0.03	10.95	
25-05-1920	23.97	-0.01	10.94		21-05-1920	25.25	-0.07	11.21	
30-08-1920	23.99	0.04	10.73		30-08-1920	25.40	0.00	10.95	
30-08-1920	24.01	0.02	10.93		30-08-1920	25.29	0.01	11.04	
15-10-1920	24.18	0.02	10.88		15-10-1920	25.23	-0.02	11.15	
15-10-1920	24.18	0.02	10.88		15-10-1920	25.33	0.04	11.03	
03-11-1920	24.16	-0.02	10.67		04-11-1920	25.36	-0.01	11.18	
03-11-1920	24.84	0.01	10.95		04-11-1920	25.26	0.03	11.06	
28-12-1920				1380	28-12-1920				1382
					28-12-1920	25.21	0.00	11.00	
					22-02-1921	24.98	0.01	10.92	
					22-02-1921	25.18	0.01	11.05	
04-04-1921	24.01	0.02	10.91		07-04-1921	25.23	0.08	10.83	
04-04-1921	23.94	0.00	10.87		08-04-1921	24.88	0.00	11.17	
25-05-1921	23.98	0.06	10.97		24-05-1921	24.92	0.04	10.86	
25-05-1921	24.01	-0.02	10.91		24-05-1921	24.94	0.00	11.13	
					18-07-1921	24.91	0.04	10.93	
					18-07-1921	24.88	0.06	11.08	
05-08-1921	24.30	0.06	10.88		05-08-1921	24.94	0.05	11.04	
05-08-1921	24.30	0.06	10.88		05-08-1921	24.94	0.05	11.04	
26-08-1921				1378					1379
25-10-1921	24.36	0.01	10.60		26-10-1921	24.84	0.03	11.11	
26-10-1921	24.27	0.01	10.94		26-10-1921	24.96	0.07	10.91	
18-11-1921	24.12	-0.04	10.58		18-11-1921	24.83	0.03	10.96	
18-11-1921	24.20	0.01	10.89		18-11-1921	25.11	0.05	10.77	
01-02-1922	23.82	-0.02	10.77		31-01-1922	25.06	-0.02	10.74	
01-02-1922	23.82	-0.02	10.77		31-01-1922	25.06	-0.06	11.04	
03-05-1922	23.94	0.05	10.92		02-05-1922	25.19	-0.03	10.92	
03-05-1922	23.92	-0.03	10.83		02-05-1922	24.91	-0.04	11.07	
26-05-1922	24.04	0.07	10.80		26-05-1922	24.97	0.04	10.85	
26-05-1922	24.28	-0.05	10.86		27-05-1922	24.64	-0.01	11.19	
28-08-1922	24.26	0.02	10.73		28-08-1922	24.38	-0.11	10.63	
28-08-1922	24.36	0.04	10.78		29-08-1922	24.66	0.01	10.90	
11-10-1922				1376					1380

Seism 32 (NS)					Seism. 31 (EW)				
Date	T [s]	μ^2	k	A [mm]	Date	T [s]	μ^2	k	A [mm]
08-11-1922	24.28	0.03	10.58		07-11-1922	25.32	0.04	11.07	
08-11-1922	24.28	0.04	10.85		07-11-1922	25.07	0.06	10.93	
06-01-1923				1376					1380
					18-01-1923	24.92	0.06	11.03	
					18-01-1923	24.98	0.02	11.00	
20-03-1923	24.36	-0.09	10.92		22-03-1923	24.68	-0.08	11.18	
21-03-1923	24.23	-0.05	11.06		22-03-1923	24.71	-0.07	11.26	
07-06-1923	23.99	0.03	11.11		06-06-1923	24.63	0.00	11.08	
07-06-1923	24.21	0.01	11.08		07-06-1923	24.98	-0.05	11.22	
12-07-1923	23.82	0.12	10.98		13-07-1923	24.63	0.07	10.78	
12-07-1923	23.99	0.01	11.00		13-07-1923	24.71	-0.02	11.18	
27-08-1923	24.21	0.01	11.09		27-08-1923	24.68	0.00	11.14	
27-08-1923	24.09	0.04	11.12		27-08-1923	24.88	0.00	11.08	
07-11-1923	23.43	0.16	10.90		07-11-1923	24.48	-0.05	11.23	
08-11-1923	24.09	-0.03	11.21		07-11-1923	24.91	0.01	11.05	
06-12-1923	24.43	-0.12	10.86		07-12-1923	25.06	-0.05	11.09	
07-12-1923	24.65	-0.02	11.09		08-12-1923	25.30	-0.03	11.15	
31-12-1923				1376					1379
12-01-1924	24.74	-0.05	10.91		11-01-1924	25.03	-0.04	11.04	
12-01-1924	24.74	-0.05	10.91		11-01-1924	25.08	-0.02	11.20	
22-04-1924	24.11	0.00	11.06		22-04-1924	24.98	0.03	11.25	
22-04-1924	24.02	-0.02	11.08		22-04-1924	24.93	0.00	11.23	
20-05-1924	23.77	0.03	11.08		20-05-1924	25.36	0.04	10.90	
20-05-1924	23.84	-0.03	11.09		20-05-1924	25.03	-0.03	11.24	
19-06-1924	23.84	0.00	11.05		19-06-1924	25.06	0.02	11.04	
19-06-1924	23.97	-0.04	11.09		20-06-1924	25.21	-0.04	11.24	
25-08-1924	23.94	-0.03	11.08		25-08-1924	25.08	-0.03	11.14	
25-08-1924	24.04	-0.02	11.06		25-08-1924	25.13	0.04	11.08	
11-11-1924	24.16	-0.01	11.03		11-11-1924	24.98	0.01	11.16	
11-11-1924	24.60	0.01	11.06		11-11-1924	24.79	0.00	11.14	
17-03-1925	22.67	0.08	10.59		11-03-1925	24.86	0.01	10.63	
17-03-1925	24.36	-0.05	10.71		11-03-1925	25.08	-0.07	11.17	
12-05-1925	25.14	-0.09	11.10		11-05-1925	25.06	-0.02	11.04	
13-05-1925	25.11	-0.04	11.12		11-05-1925	25.08	-0.05	11.24	
29-06-1925	24.75	0.04	11.03		29-06-1925	25.43	0.02	10.64	
29-06-1925	24.72	-0.03	11.10		29-06-1925	25.21	-0.01	11.25	
29-07-1925	24.43	0.04	11.09		29-07-1925	24.86	0.06	10.98	
29-07-1925	24.43	0.04	11.09		29-07-1925	24.86	0.06	10.98	
01-10-1925	23.97	0.03	11.01		02-10-1925	24.83	-0.01	11.23	
03-10-1925	24.28	0.09	10.98		02-10-1925	25.06	0.02	11.05	

Seism 32 (NS)					Seism. 31 (EW)				
Date	T [s]	μ^2	k	A [mm]	Date	T [s]	μ^2	k	A [mm]
18-11-1925	24.28	0.07	10.67		18-11-1925	24.68	-0.03	11.25	
18-11-1925	24.80	0.02	11.14		19-11-1925	25.13	0.01	11.09	
02-02-1926	24.69	0.02	11.14		01-02-1926	24.98	-0.03	11.11	
02-02-1926	24.75	0.03	11.08		01-02-1926	24.98	-0.03	11.11	
13-04-1926	24.16	0.05	11.07		12-04-1926	24.93	0.05	10.85	
13-04-1926	24.72	-0.03	11.13		12-04-1926	25.03	-0.03	11.18	
16-06-1926	23.87	0.14	10.96		15-06-1926	23.86	0.12	10.97	
17-06-1926	23.94	-0.01	10.96		19-06-1926	24.23	0.02	11.11	
04-08-1926	22.74	0.21	10.68		04-08-1926	23.71	0.16	10.83	
04-08-1926	24.15	0.01	11.04		05-08-1926	25.23	0.07	10.79	
21-10-1926	23.25	0.13	10.58		21-10-1926	26.36	-0.15	11.20	
22-10-1926	24.92	0.05	10.95		21-10-1926	25.30	0.00	11.12	
22-12-1926	23.82	0.05	10.62		22-12-1926	25.26	-0.02	11.04	
23-12-1926	23.99	-0.01	10.85		22-12-1926	25.43	0.03	11.02	
25-03-1927	23.92	-0.01	10.80		25-03-1927	25.13	0.04	11.03	
25-03-1927	24.69	0.00	10.89		25-03-1927	25.11	-0.01	11.23	
13-06-1927	24.14	0.10	10.93		14-06-1927	25.18	0.04	11.08	
13-06-1927	24.80	0.00	11.07		14-06-1927	25.16	-0.04	11.19	
11-08-1927	24.16	0.13	10.91		11-08-1927	25.21	0.08	10.72	
11-08-1927	24.14	0.13	10.89		11-08-1927	25.26	0.04	11.04	
13-08-1927	24.14	0.07	10.86						
11-11-1927	24.01	0.06	10.44		11-11-1927	24.83	0.02	11.10	
11-11-1927	24.16	0.05	10.84		12-11-1927	25.11	0.02	11.03	
13-12-1927	24.01	-0.01	10.71		14-12-1927	24.98	-0.05	11.24	
14-12-1927	24.52	0.06	11.11		14-12-1927	25.16	0.02	11.05	
27-02-1928	24.50	0.07	11.05		27-02-1928	25.16	0.04	11.08	
27-02-1928	24.43	0.02	11.06		27-02-1928	25.01	0.00	11.20	
08-06-1928	24.23	0.10	11.04		08-06-1928	25.26	0.03	10.83	
08-06-1928	24.21	0.01	11.11		08-06-1928	25.18	-0.02	11.16	
17-08-1928	24.18	0.07	11.05		17-08-1928	25.33	0.09	10.92	
17-08-1928	24.18	0.07	11.05		17-08-1928	25.33	0.09	10.92	
07-11-1928	24.63	-0.02	11.05		08-11-1928	25.13	-0.01	11.17	
07-11-1928	24.50	0.06	11.06		08-11-1928	25.30	0.05	11.04	
19-12-1928	24.23	-0.04	11.11		20-12-1928	24.43	0.05	10.96	
19-12-1928	24.45	0.01	11.13		20-12-1928	25.11	0.02	10.98	
15-02-1929	24.89	-0.01	10.47		15-02-1929	25.16	-0.04	11.14	
15-02-1929	24.45	-0.02	11.07		15-02-1929	25.18	-0.04	11.14	
06-05-1929	24.11	0.06	11.06		30-04-1929	25.26	0.02	10.90	
06-05-1929	24.04	0.01	11.08		30-04-1929	25.38	-0.05	11.18	
31-05-1929	24.04	0.12	10.87		31-05-1929	25.60	0.10	10.19	

Seism 32 (NS)					Seism. 31 (EW)				
Date	T [s]	μ^2	k	A [mm]	Date	T [s]	μ^2	k	A [mm]
01-06-1929	24.60	0.02	11.01		31-05-1929	25.28	-0.01	11.22	
20-08-1929	24.11	0.07	11.02		20-08-1929	25.38	0.00	11.06	
20-08-1929	24.11	0.07	11.02		20-08-1929	25.38	0.00	11.06	
31-10-1929	24.06	0.03	10.90		31-10-1929	25.33	-0.04	11.17	
31-10-1929	24.41	0.06	11.06		31-10-1929	25.28	0.05	10.97	
30-01-1930	24.14	0.03	10.89		29-01-1930	25.08	0.06	10.74	